

Biological Synthesis and Structural Characterization of Selenium Nanoparticles and Assessment of Their Antimicrobial Properties

Bahig El-Deeb^a, Abdullah Al-Talhi^b, Nasser Mostafa^c, Rawan Abou-assy^{d*}

^aFaculty of Science, Botany Department, Sohag University, Sohag, Egypt

^{b,c,d}Faculty of Science, Biology Department, Taif University, Taif, KSA

^aEmail: b.aldeeb@tu.edu.sa

^bEmail: altalhi@tu.edu.sa

^cEmail: n.mostafa@tu.edu.sa

^dEmail: Rawan.assi@hotmail.com

Abstract

Biological synthesis of selenium nanoparticles (SeNPs) using microorganisms has received profound interest because of their potential to synthesize nanoparticles of various size, shape and morphology. In the current study, 206 selenium resistant bacterial isolates were isolated from 18 samples from different environmental sources of Saudi Arabia. Among These isolates, bacterial strain BGRW was selected on the basis of its ability to produce stable extra/intracellular SeNPs. Molecular characterization of this isolate indicated that BGRW strain belongs to the *Providencia vermicola*. BGRW was found to be highly resistant to selenium dioxide up to 20 mM. The biosynthesis of SeNPs was monitored by UV-Visible spectrum that showed surface plasmon resonance (SPR) peak at 295 nm. Further characterization of synthesized SeNPs was carried out using the XRD, TEM and FTIR spectroscopy. TEM and XRD analysis revealed that the SeNPs synthesized by BGRW was hexagonal in shape with a size range of ~3 to 50 nm with average 28nm. FTIR spectroscopy confirmed the presence of proteins as the stabilizing agent surrounding the nanoparticles. In the present study six antibiotics were investigated to explore their synergistic effect when combined with SeNPs against various pathogenic. All tested antibiotics showed synergistic inhibition against a growth of the pathogenic bacteria. The biocide actions of SeNPs on Gram-negative and Gram-positive pathogens were studied using SEM. The results showed damage, blebs, fusion, clumps and randomly distribution in the cell wall of the tested microbes resulting the death of cells.

* Corresponding author.

The MIC 90 of SeNPs was 10µg/mL, 15µg/mL and 20µg/mL for *Staphylococcus aureus*, *Bacillus cereus* and *Escherichia coli* respectively. The effect of SeNPs on the prevention and removing of biofilm were also studied, the antibiofilm concentration of SeNPs was 12µg/mL against *Salmonella enteritidis* and *B. cereus*, 16µg/mL against *S. aureus* and *E. coli* while the antibiofilm concentration was 18µg/mL against *Proteus sp.* and *Pseudomonas aeruginosa*. Although the biogenic SeNPs had antimicrobial and antibiofilm effects, they did not show significant ability to remove the established biofilm up to 32µg/mL. The concentration of 24µg/mL showed a slight effect on removing the established biofilm. The antibiofilm effect of the combination of SeNPs with amoxicillin was investigated against six bacterial biofilms and result show a synergistic effect at a lower than the antibiotic or SeNPs minimum antibiofilm concentrations.

Keywords: Selenium nanoparticles; Antimicrobial effect; MIC; 16s rRNA; Antibiofilm; Transmission electron microscope; X-ray; FTIR analysis.

1. Introduction

Nanotechnology provides a valid tool to give effect enhancing and toxicity reducing of many chemo-preventive compounds that naturally occurring, like elemental selenium [1]. The synthesis of nanoparticles which have sizes less than 100 nm in at least one dimension with unique chemical, physical [2], photoelectrochemical [3], electrical, mechanical, electronic [4], magnetic [5], optical [6] and biological properties [7] that dissimilar from those of the bulk materials.

The origin of "Selenium" name came from the Selene which means moon goddesses in a Greek culture. Selenium (Se) was discovered by Jacob Berzelius in 1818. This element can be considered an essential trace element micronutrient for living creatures at low concentrations but it becomes toxic and harmful at higher doses. The range of dietary deficiency (< 40 µg/day) and excess (> 400 µg/day) is fairly narrow [8]. There are over 40 diseases in man is known to be related to selenium deficiency [9]. In general, selenium occurs in large amounts in coals and crude oils but it exists comparatively in little amounts in geological raw materials, soils and sediments [10]. In addition, industrial products such as oil refining, phosphate and metal ore mining and coal fire-based power activity can all participate in the dispersion of selenium in the earth. [11]. All of which ensure possible ways for the mobilization of selenium in the biosphere. Selenium exists in four valence states: selenate (Se^{+6}), selenite (Se^{+4}), selenide (Se^{-2}) and elemental selenium (Se^0) and can combine with oxygen, sulfur, halogens and metals [12]. These compounds are metabolized in the living system [13, 14]

Chemical and physical production of SeNPs are expensive, contamination arises from chemical precursors and products, high toxicity of the used solvents and in many cases demand specialized equipment [15, 16]. The main disadvantages of physical methods are their low production rates, high energy consumption and high costs [16]. Biological methods of nanoparticles synthesis are considered to be safe and called "green chemistry" as they tend to be an environmentally friendly method for production of SeNPs because they include natural processes that happen in living systems [17]. Microorganisms act a major part in the biogeochemical cycle of selenium in the environment [18] including anaerobic selenite reducing bacteria encompass *Thauera selenatis* [19], *Aeromonas salmonicida* [20] and purple non-sulfur bacteria [21] and aerobic bacteria involved in selenite

reduction include diverse species such as *Rhizobium sp.* B1 [22], *Stenotrophomonas maltophilia* SeITE02 [23], *Pseudomonas sp.* CA5 [24], *Duganella sp.* and *Agrobacterium sp.* [25]. However, these methods also have some drawbacks, this limitation has been overcome by optimizing the growth condition for the microorganisms through the adjustment of factors such as the pH [26], incubation time and temperature [27], metal salt concentrations [28] and the amounts of biological inoculum [29]. It should be noted that SeNPs as the reverse reaction is too slow to form Se compounds [25]. Metal ions are often absorbed into the cells, reduced and deposited in intracellular space of microorganisms to form NPs [30]. Not only intracellular but also extracellular elemental selenium formation was detected, although accumulation of SeNPs was mainly observed inside the bacterial cell [31]. Biosafety assessment of SeNPs did not show considerable toxicological effects on *Artemia larvae* [32]. The acute toxicity (LD50) of SeNPs in mice (92.1 mg/kg) is remarkably lower than that of selenite (15 mg/kg), selenomethionine (25.6 mg/kg) and methylselenocysteine (15 mg/kg) [33]. Limited information about the inhibitory effect of SeNPs on the prokaryotic organisms is obtainable [34]. Reference [35] demonstrated that selenium-enriched probiotics highly inhibit the growth *in-vivo* and *in-vitro* of pathogenic *E. coli*. While [36] demonstrated that SeNPs showed good antimicrobial activity against *Pseudomonas sp.* than *Staphylococcus aureus*, but SeNPs failed to show activity against *E. coli* and *Klebsiella sp.*. Even so at high concentration (620 µg/mL), selenium nanoparticles inhibited the growth of *S. aureus* and *E. coli* [37]. Recently, the biosynthesized SeNPs were used to prevent growth and biofilm formation by six foodborne pathogens including *Bacillus cereus*, *Enterococcus faecalis*, *S. aureus*, *Escherichia coli* O157:H7, *Salmonella Typhimurium*, and *Salmonella Enteritidis*. The MIC90 of SeNPs against all tested bacteria was 25µg/mL, whereas the antibiofilm concentration was 20µg/mL against all bacteria, except *B. cereus* [32]. Chemically produced SeNPs with range of 40-100 nm showed inhibition effect against *S. aureus* when it used at concentrations of 7.8, 15.5 and 31 µg/mL, they added that there is no variation between the effects of these concentrations, when SeNPs were applied at concentrations higher than 20 µg/mL against the Gram-positive and Gram-negative pathogenic bacteria, no considerable differences were obtained between all studied strains at the same concentration [34]. SeNPs were synthesized by *Lactobacillus sp.* or their cell-free spent broth inhibited the growth of *Candida albicans* and they recommended investigating for possible use in anti-Candida probiotic formulations [38]. On the contrary, a stimulating activity appeared in a sub-inhibitory concentration of SeNPs (2.5-10 µg/mL) to enrichment some organisms such as *Aspergillus niger* [39].

In this study, we report the (I) biosynthesis of SeNPs using *Providencia vermicola* BGRW strain which isolated from the rhizosphere of the farm at Taif, KSA. (II) Characterization of biogenic SeNPs by UV-Vis spectroscopy, transmission electron microscopy (TEM), Fourier transforms infrared spectroscopy (FTIR) and X-ray diffraction (XRD) spectra. (III) Investigation of the effect of SeNPs against some pathogenic microorganisms on planktonic and biofilm forms and (IX) in addition to the synergistic effect of SeNPs combined with antibiotics.

2. Materials & Methods

2.1. Chemicals

Media and solvents were purchased from Sigma Aldrich Co., Oxoid-England, DIFCO-BD and Pharmacia

Chemicals and kits implicated in molecular biology tests (PCR product purification kit, Hot Star Master mix kit and DNA marker) were obtained from QIAGEN, All chemicals were at least of analytical reagent grade. The bacterial pathogens were obtained from Al-Idwani Hospital, Taif, KSA. Milli-Q deionized water was used throughout the experiments.

2.2. Bacterial Strain and Growth Conditions

2.2.1. Isolation of selenium reducing bacteria

The soil samples were transferred to the laboratory in sealed plastic bags and kept at 4°C until further use while water sample was collected in lab bottles. Samples were serially diluted in sterile 0.8% NaCl solution and then plated onto agar plates with different concentrations of selenium dioxide and incubated for 2 days at 37 °C. Colonies which have red color were evaluated as selenium reducing strains. Previously isolated strains were grown on tryptic soy agar (TSA), casein starch agar for actinomycetes or marine agar for halophilic bacteria [40]. After isolation, the strains were maintained in slant agar amended with 0.1 mM selenium dioxide at 4°C for further studies.

2.2.2. Screening of isolates for SeNPs Synthesis

Selenium reducing strains especially were tested for the synthesis of selenium nanoparticles. Bacterial strains were grown up in test tubes containing 10 ml tryptic soy medium supplemented with 1mM SeO₂ in a shaker incubator at 37°C After 24 h incubation, the biomass was separated from the medium by centrifugation (7000 rpm, 10 min) and the red selenium nanoparticles formed were inspected in the precipitated biomass or extracellular formation of SeNPs in the upper supernatant according to [41] with slight modification. The accumulation and reduction of selenium were followed by visual observation of the biomass turning red, as a convenient indication of the formation of SeNPs [31].

2.2.3. Collection and purification of selenium nanoparticles

SeNPs collection was different depending on NPs location when cells containing the particles as intracellular production, bacteria were collected by centrifugation (7000 rpm, 4°C, 10 min) from 50 mL amended with 1mM SeO₂ of the culture and washed three times with ultrapure water. Subsequently, the pellet was resuspended in 5 mL of Phosphate Buffer solution pH. 7.2 as wash buffer and followed by cell-disruption with an ultrasonicator (130 W, 10 min, Vibracell VCX- 130; Sonics and Materials Inc., CT, USA). The suspensions were filtered with 0.25 µl Millipore syringe filters. Then the SeNPs were collected from the filtrates by centrifugation (10,000 rpm, 4 ° C, 30 min) and suspended in 5 mL of ultrapure water according to [42] with slight modification. When the production of SeNPs was extracellular, bacteria were precipitated using centrifugation (7,000 rpm, 4°C, 10 min) from 50 mL of the culture then the supernatant was filtered through 0.25 µl Millipore syringe filters to obtain free cell supernatant which had SeNPs. Then the SeNPs were collected using centrifugation (10, 000 rpm, 4 ° C, 30 min) and suspended in 5 mL of ultrapure water [43]. The precipitate of SeNPs from intra/extracells was washed with ethanol and water to remove if any contaminants present and dried in hot air oven at 45° -50°C this step called purification [44]. The selenium nanoparticles were purified from the protein and other

contaminants.

2.2.4. Genotypic characterization of *Providencia vermicola* BGRW

The morphological and physiological characterization of the selected isolates were performed by biochemical tests using the Bergey's Manual of Determinative Bacteriology [45]. Further characterization of target isolate was done by means of 16S rRNA gene analyses. The genomic DNA of the isolate was extracted according to the standard method. The 16s rRNA gene was amplified by PCR using the universal primer set 8–27F 5'-GAGTTTGATCCTGGCTCAG-3' [46] and 1492R 5'-GGTTACCTTGTTACGACTT-3' [47]. The conditions for thermal cycling were as follows: denaturation of the target DNA at 94 ° C for four minutes, followed by 30 cycles at 94 ° C for one minute, primer annealing at 52 ° C for one minute, and primer extension at 72 ° C for one minute. At the end of the cycling, the reaction mixture was held at 72 ° C for 10 min and then cooled to 4 ° C. The amplified PCR product was sequenced using big dye terminator cycle sequence kit. PCR products were cloned into MacroGen Vector DB through the Easy T-Vector System. The product of the sequencing reaction was analyzed by using DNA sequencer ABI PRISM 310 genetic analyzer (Perkin Elmer, USA). This step was conducted by (MacroGen, Korea). Data were submitted to Gen Bank database and 16s rRNA gene sequence was registered as accession KX447430 in the GenBank database.

The comparison of 16s rRNA gene sequences is a powerful tool for deducing phylogenetic and evolutionary relationships among bacteria, archaeobacteria and eukaryotic organisms. The DNA sequence was compared to the Gen Bank database in the National Center for Biotechnology Information (NCBI) using the BLAST N program [48]. These sequences were aligned using the CLUSTAL_W 1.83 program [49] and a neighbor-joining phylogenetic tree was constructed using MEGA 7.0.14. Program against the database of type strains with validly published prokaryotic names as illustrated by [50]. Missing nucleotides at both the beginning and the end of the sequences were deleted before construction of the trees.

2.3. Characterization of selenium nanoparticles

2.3.1. UV-Vis spectrophotometer

The characterizations of the synthesized nanoparticles were carried out according to the method described previously [51]. The biologically synthesized selenium nanoparticles were characterized by UV-Vis spectroscopy (Perkin Elmer, Lambda 25) instrument scanning in the range of 200-800 nm, at a resolution of 1 nm. Sample for UV-Vis spectra measurement was conducted to collected and purified SeNPs as mention above at 25°C, cell-free supernatant without the addition of SeO₂ was used as a control throughout the experiment.

2.3.2. Transmission Electron Microscopy (TEM) measurements

The SeNPs sample was first centrifuged at 10,000 rpm for 10 minutes. For transmission electron microscope (TEM) measurements, a drop of solution containing synthesized selenium nanoparticles was placed on the carbon coated copper grids and kept under vacuum desiccation for an overnight before loading them onto a specimen holder. Study of size and morphology of the nanoparticles was performed by means of transmission

electron microscopy (TEM) operated at 120 k accelerating voltage (JTEM 1230, Japan, JEOL) at King Saud University.

2.3.3. X-Ray Diffraction (XRD) analysis

X-ray diffraction (XRD) analysis was carried out using an automated diffract meter (Philips type: Pw1840), at a step size of 0.02, the scanning rate of 20 in 2θ /min, and a 2θ range from 10° to 80° . Indexing of the powder patterns and least squares fitting of the unit cell parameters was possible using the software X'Pert High score Plus.

2.3.4. Fourier Transforms Infrared Spectroscopy (FTIR) analysis

FTIR measurements were carried out using Attenuated Total Reflection Fourier Transform Infrared (ATR-FTIR) spectrometer (Bruker, Germany, Alpha-P). The instrument was configured with ATR sample cell including a diamond crystal with a scanning depth up to 2 micrometers. To separate any free biomass residue or compound that is not capping ligand of the nanoparticles, the residual solution of 100 ml after the reaction was centrifuged at 10000 rpm for 30 min. The bio-transformed products present in the cell-free filtrate were freeze-dried sample powders were applied to the surface of the crystal then locked in place with a "clutch-type" lever before measuring transmittance. Each of the spectra was collected in the range 400- 4,000 cm^{-1} at 2 cm^{-1} resolution. Comparing with the conventional transmission mode, this technique is faster sampling without preparation, excellent reproducibility and uncomplex to use.

2.4. Antimicrobial activity of selenium nanoparticles

2.4.1. Determination the inhibition zone of SeNPs different concentrations

The antimicrobial activity of selenium nanoparticles were assessed by well diffusion method (Kirby-Bauer testing) according to [52] with slight modification, against Gram-positive pathogens (*Staphylococcus aureus*, *Bacillus cereus*, *MRSA*, *Streptococcus pneumoniae* and *Streptococcus agalactiae*), Gram-negative pathogens (*Escherichia coli*, *Pseudomonas aeruginosa*, *Enterobacter sp.*, *Enterococcus sp.*, *Proteus mirabilis*, *Klebsiella sp.*, *Salmonella enteritidis* and *Stenotrophomonas maltophilia*) and *Candida albicans* which were obtained from the microbiology laboratory of Al-Idwani Hospital. The Muller-Hinton agar plates were prepared and 100 μl of each activated culture of pathogens were spread to individual plates by sterile swab. Wells of 6 mm diameter were made using a sterile cork borer and different concentrations (10 or 15 $\mu\text{g}/\text{ml}$) of SeNPs were added into individual wells and incubated at 37°C for 24 h and the Zone of Inhibition (ZOI) formed surrounding the well was noted for all strains. Clear zone of ($25 \leq \text{ZOI} \leq 40$ mm) in diameter were classified as (very strong inhibition), zone of ($15 \leq \text{ZOI} < 25$ mm) in diameter were classified as (strong inhibition), zone of ($10 \leq \text{ZOI} < 15$ mm) in diameter were classified as (moderate inhibition) and < 10 as (weak inhibition) (Elert and Juttner, 1996). The zone of inhibition was compared against a set of standard antibiotics discs: norfloxacin (NX) $10\mu\text{g}$, ampicillin (AMP) $25\mu\text{g}$, sulfamethoxazole (SXT) $25\mu\text{g}$, penicillin V (PNV) $10\mu\text{g}$, penicillin G (PNG) $10\mu\text{g}$ and gentamicin (GN) $10\mu\text{g}$.

2.4.2. Synergistic effect of SeNPs with an antibiotic at an antibacterial activity

The disk diffusion method was used to evaluate the synergistic of SeNPs with antibiotics. Briefly, Mueller-Hinton agar plates were inoculated with 100 µl of each activated culture of pathogens and made three discs in each plate; the first for 100µl of SeNPs, the second for antibiotic (HiMedia Chemicals Pvt. Ltd., Mumbai, India), the third for combination of SeNPs + antibiotic and were incubated at 37°C for 24 h. Next, the inhibition zone (ZOI) diameters of them were measured. Synergistic effect was calculated by the following equation: The synergistic effect = $\frac{(B-A)}{(A)} \times 100$ where A is ZOI for the antibiotic and B is ZOI for the antibiotic + SeNPs [53].

2.4.3. Determination minimum inhibition concentration (MIC 90) of SeNPs by plate counting method

Determination of (MIC 90) which defined as minimum inhibitory concentration required to inhibit the growth of 90% of organisms by colony forming unit (CFU) to pathogens treated with SeNPs by plate counting method. Antibacterial test pathogens were grown in LB liquid medium at 37°C for 12 hours before they were diluted in fresh LB liquid medium to reach OD₆₀₀ = 0.003 (optical density). Gradient concentrations of SeNPs (5, 10, 15, 20, 25 µg/ml) were then added to the culture medium. Bacteria and SeNPs mixed cultures were put into a 37°C incubator for 24h. Serial 10-fold dilutions with saline were then made and cultured on LB agar plates. Plates were incubated overnight at 37°C and CFU was determined using the conventional plate count method. SeNP-free pathogen was used as a negative control and 25 µg/ml sulfamethoxazole was used as a positive control for antibacterial activity [54].

2.4.4. Assay of the effect of SeNPs on bacterial cell structure by Scanning Electron Microscopy (SEM)

The interaction between pathogenic isolates and the potentially effective SeNPs was examined by Scanning electron microscopy (SEM). Muller-Hinton broth was prepared and sterilized to use for preparing the inoculums. After the incubation period, 100 µl of the bacterial cultures were added in a sterilized tube and incubated with 25µg/mL of SeNPs for 6 h at 37 °C. Control group was generated without any NPs After that 0.1 ml of treated and untreated cells were added to sterile blank discs and left to dry for morphology and structure analysis by SEM according to the method that described by [55] with slight modification.

2.4.5. Antibiofilm effect of SeNPs

The antibiofilm effect of SeNPs against various pathogens was determined in vitro using the commonly used 96 wells polystyrene microtiter-plates method (Khirallah and El-deeb, 2015). Briefly, 10 µL activated culture of each tested strain (about 10⁶ CFU/mL) was added. The final tested concentrations of SeNPs were 0, 4, 8, 12, 16 and 18µg/ml. The total volume in each well was adjusted to 250 µL using tryptic soy broth (TSB). Wells contained 240 µL TSB and 10 µL stimulated culture were used as positive control, whereas wells with 250 µL TSB were applied as a negative control. Plates were incubated at 37°C for 24 h. After the incubation period, contents of the microtiter-plates were emptied and the wells were washed three times with 300 µL of phosphate buffered saline (PBS, pH 7.2). The remaining adhered bacteria were fixed with 250 µL of methanol per well. After 15 min, microtiter plates were poured off and air dried. The microtiter-plates were stained with 250 µL per

well of 1% crystal violet, used for gram-staining, for 5 min. The surplus of stain was rinsed off by placing the microtiter-plates under slow running tap water. After drying the microtiter-plates, the dye bound to the adherent cells was extracted with 250 μL of 33% (v/v) glacial acetic acid for each well. The absorbance (A) of each well was measured at 570 nm using an ELISA reader (HumaReader HS, Human, Germany). The cut-off absorbance (A_c) was the mean absorbance of wells contained TSB only, without bacterial cells (negative control). Based on the absorbance ($A_{570\text{nm}}$) obtained after 24 h by bacterial biofilms, strains were classified into four categories [56, 57]. Briefly, Strains were classified as follows: $A = A_c$ = no biofilm producer (-); $A_c < A \leq (2 \times A_c)$ = weak biofilm producer (+); $(2 \times A_c) < A \leq (4 \times A_c)$ = moderate biofilm producer (++); $(4 \times A_c) < A$ = strong biofilm producer (+++). All tests were implemented in triplicate and the results were averaged. The antibiofilm concentration was defined here as the minimum SeNPs concentration that caused restrain biofilm formation by each tested bacterium (to be in the category of no biofilm producer). The percentage of biofilm inhibition was calculated using the equation:

$$\% \text{ biofilm inhibition} = 1 - (\text{OD}_{570} \text{ of cells treated with SeNPs} / \text{OD}_{570} \text{ of non-treated control}) \times 100.$$

2.4.6. Biofilm removing ability of SeNPs

The established biofilms by the tested strains were developed as mentioned above. To investigate the ability of SeNPs to remove the established biofilms, different concentrations (0, 20, 24, 28 and 32 $\mu\text{g/ml}$) of SeNPs were incorporated in the PBS that was used in the washing step as described by [32]. After incubation for 24 h at 37°C contents of the microtiter-plates were poured off and the wells were washed three times with 300 μL of PBS that contained the tested concentration of SeNPs. The remaining steps were done as mentioned above and the pathogenic strains were classified (no-, weak, moderate or strong biofilm producer) based on the quantity of biofilm remained after washing with SeNPs.

2.4.7. Synergistic antibiofilm effect of SeNPs with antibiotic

Synergistic antibiofilm effects of SeNPs with antibiotic against various pathogens were determined also in vitro using the commonly used 96 wells polystyrene microtiter-plates method. Briefly, 10 μL activated culture of each tested strain (about 10^6 CFU/mL) were added. The final tested concentrations of SeNPs were 7.5, 10, 12.5, 15, 17.5, 20 and 25 $\mu\text{g/ml}$ with the same concentrations (7.5, 10, 12.5, 15, 17.5, 20 and 25 $\mu\text{g/ml}$) of amoxicillin antibiotic (AMC) that means we used (15, 20, 25, 30, 35, 40 and 50 $\mu\text{g/ml}$) concentrations of 1(SeNPs):1(AMC). The effect of only amoxicillin on biofilm forming ability of all tested strains was determined by using (15, 20, 25, 30, 35, 40 and 50 $\mu\text{g/ml}$) concentrations as a control. The total volume in each well was adjusted to 250 μL using tryptic soy broth (TSB). The remaining steps were done as mentioned above.

3. Results & Discussion

3.1. Isolation of selenium reducing bacteria

Eighteen samples were collected from different areas as follows: 4 samples of soil from rhizosphere of plant irrigated with waste water from farm at Taif ,1 sample of soil from Al-Sail roadway at Taif , 2 samples of soil

from rhizosphere at Taif University , 4 samples of soil from rhizosphere at Makkah city , 2 samples of metal-rich dump soil at industrial city, Taif , 1 sample of soil from drainage of chemical labs at Taif University , 1 sample of soil from Al-Arj Valley at Taif , 1 sample of *Calotropis procera leaf* surface, 1 sample of waste water and 1 sample of Red- sea water from Jeddah coast, during an exhaustive screening program, undertaken in our laboratory to isolate bacteria capable of synthesizing selenium nanoparticles. The samples were not chosen randomly, but sites of isolation measured way based on increasing the amount of pollutants that were exposed to the region and the nanoparticles producing bacteria isolating places in previous studies [58]. The collected samples were serially diluted and plated on tryptic soy agar (TSA) medium supplemented with 1mM SeO₂ and the plates were incubated at 37 °C for 48 h. After the incubation period the bacterial colonies were observed and they were further subcultured on the same medium to obtain pure colonies tolerate selenium ions. It is known that the physical properties of biologically produced nanoparticles may vary among different types of organisms [59, 60]. In this study, varieties of bacteria were screened for their ability to synthesis intra/extracellular selenium nanoparticles of uniform size and shape. The study indicated that terrestrial strains isolated from soil irrigated with wastewater produced the nanoparticle faster than others strains. Rest of the study reported in this work was done using the SeNPs synthesized using the cultures of Gram-negative, facultative anaerobic, straight rods and motile that highly resistant to selenium dioxide reach to 20 mM which was later identified as *Providencia vermicola* BGRW belonging to the family *Enterobacteriaceae* which has discriminatory ability to tolerate many metals such as Selenium, Cadmium, Silver, Zinc, Copper, Lead, Nickel, Cobalt and Bismuth metals.

3.2. Phylogenetic analysis of 16s rRNA gene sequence

Molecular characterization of bacterial strains using 16s rRNA gene study is an essential method used for taxonomic purposes, largely due to the mosaic composition of phylogenetically conserved and variable regions within the gene [61, 62]. Molecular techniques were used to prove and further confirm the identification of the *Providencia* strain BGRW to the species level. The 16s rRNA gene phylogeny was carried out, DNA was extracted from bacterium *Providencia* strain BGRW according to [63]. An amplicon representing the 16s rRNA gene of 799bp was obtained. The partial 16s rRNA gene sequence was determined and was compared to the Gen Bank database in the National Center for Biotechnology Information (NCBI) using the BLASTN 2. 4. 0, CLUSTAL W and the MEGA 7 program to Phylogenetic tree analysis. This isolate was found belonging to the *Providencia* species with homology level (99%) as depicted in the Phylogenetic tree analysis (Figure.1). It was identified as *Providencia vermicola* by alignment our sequence to sequence of *Providencia vermicola* strain CICRSPBB. This strain was isolated from the rhizosphere of plant irrigated with waste water from Farm at Taif, Saudi Arabia. The bacterial strain, *Providencia vermicola* BGRW which was isolated in the present study appears to be a promising organism to meet the need for the production of original selenium nanoparticles based wound ointment, anticancer drug and as a better coating agent in medical instruments, greater studies are requirement to quantify these observed effects of SeNPs.

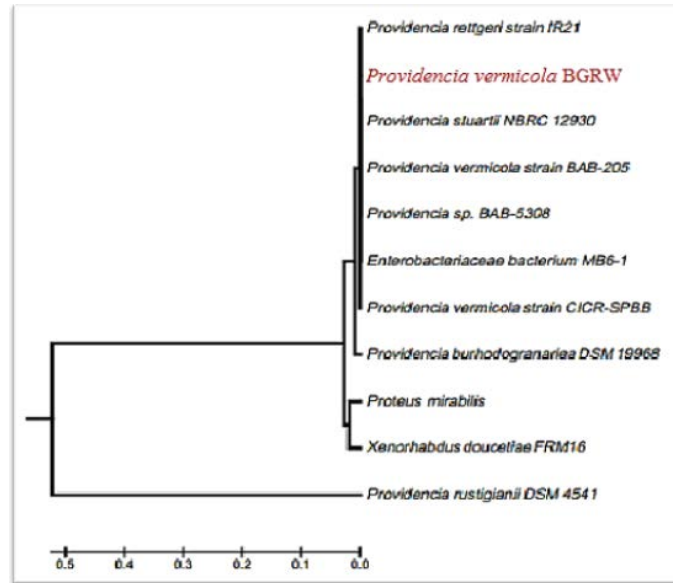


Figure 1: Phylogenetic tree based on 16s rRNA gene sequence comparisons of *Providencia vermicola* BGRW, using neighbor joining tree method, maximum sequence difference=0.5.

3. 3. Characterization of selenium nanoparticles

3.3.1. Visualization of biogenic selenium nanoparticles color

Visual observation of the culture incubation with selenium dioxide at 37° C for 24 h in dark showed a color change from light yellow to bright red indicating the formation of red-colored elemental Se (Figure. 2, tube.1), which are the characteristic of selenium nanoparticles formation [25]. This red color due to the excitation of surface plasmon vibrations of selenium nanoparticles provides a convenient spectroscopic signature of their production [25] whereas no color change could be demonstrated in a solution of selenium dioxide as a negative control (Figure. 2, tube.2). Many related studies revealed that metal reduction and precipitation might involve a complex of either reductases, capping proteins, quinones or cytochromes, electron shuttles or phytochelatin that are known to reduce and stabilize various metal, metal oxides and metal sulfide nanoparticles [25].

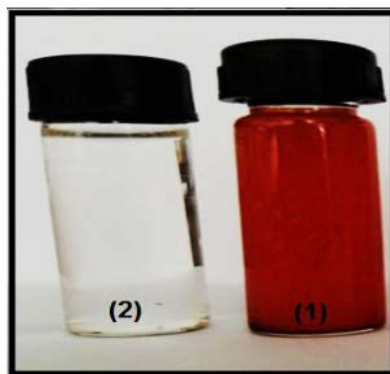


Figure 2: A photograph showing the red selenium nanoparticles in a tube (1) and no color change at negative control in a tube (2).

3.3.2. UV-Vis spectrophotometer for selenium nanoparticles

For SeNPs spectra measurements, the UV-Vis spectrum illustrated shows an absorption peak in the region of 200-800 nm for the cell filtrate from the culture of *Providencia vermicola* BGRW strain which had 1mM of SeO_2 as a source of selenium ions, a well-defined absorption peak at ca. 295 nm appears in (Figure. 3) that corresponds to the wavelength of the surface plasmon resonance (SPR) of selenium nanoparticles [64]. Various reports have confirmed that the resonance peak of selenium nanoparticles appears around this region, but the accurate position depends on several factors such as particle's size, shape, and material composition, as well as the local environment [65]. There were a lot of study about SeNPs formation have various absorption peaks in UV-vis spectra indicate to a presence of SeNPs. In these studies, the peaks appeared at 290 nm [66], strong absorption band located at 265 nm [41, 67] and the peak was seen at around 263 nm [32]. While the UV-Visible absorption spectra of SeNPs recovered from the culture broth gave a characteristic peak at 590 nm which corresponds to the large particle size of 182.8 ± 33.2 nm [68].

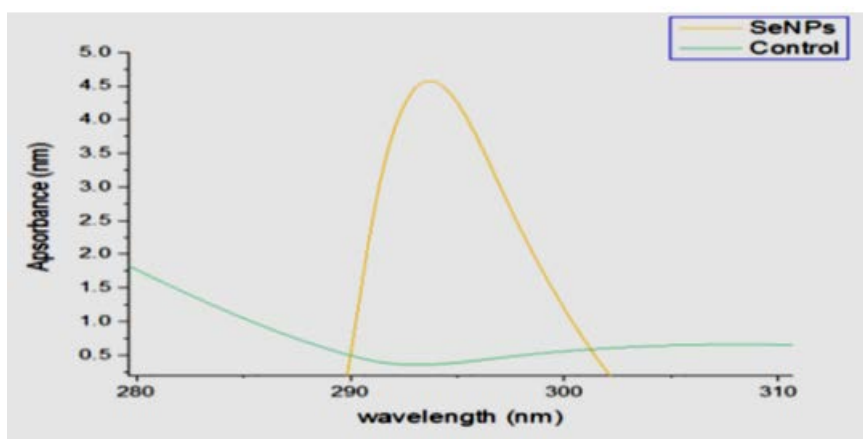


Figure 3: UV-Vis spectra recorded of selenium nanoparticles produced by *Providencia vermicola* BGRW, The absorption spectrum of SeNPs exhibited a strong peak at 295 nm and the observation of such band is assigned to surface plasmon resonance of the particles and UV-spectra of cell-free supernatant was also represented as a control.

3.3.3. Transmission Electron Microscopy (TEM) measurements of selenium nanoparticles

TEM images of the selenium nanoparticles synthesized by *Providencia vermicola* BGRW and the particle size distribution histogram of selenium particles were done. Figure 4 demonstrated the related particle size histogram obtained after measuring 78 particles from culture of *Providencia vermicola* BGRW with 1mM SeO_2 at pH 7.0 under 37 °C incubation for 24 h, the particles ranged in size approximately from 3 to 50 nm in diameter and possessed an average size of 28 nm (\pm SD) under aerobically condition. It has been reported that the particle size is decreased in presence of O_2 , it is obvious that oxygen will promote oxidation of selenium as a consequence of which the redox step becomes slower producing smaller selenium nanoparticles [69]. Also, transmission electron micrographs of the prepared selenium nanoparticles (Figure. 4) showed that the particles were hexagonal monodispersed nanoparticles, the nanoparticles were not in direct touch even within the aggregates,

point out to stabilization by a capping protein/peptide. Many of the previous studies showed selenium nanoparticles synthesis by bacteria but the disadvantage was large-size of particles which were SeNPs with 100 to 550 nm, with an average size of 245 nm were produced [41], 50 to 400 nm spherical SeNPs [70], *Lactobacillus acidophilus* produced 50-500nm SeNPs, *Bifidobacterium sp.* produced 400-500 nm SeNPs and *Klebsiella pneumoniae* produced 200-300nm SeNPs [71] comparing with small size were obtained by plant extract like Dried *Vitis vinifera* (Raisin) Extract produced.

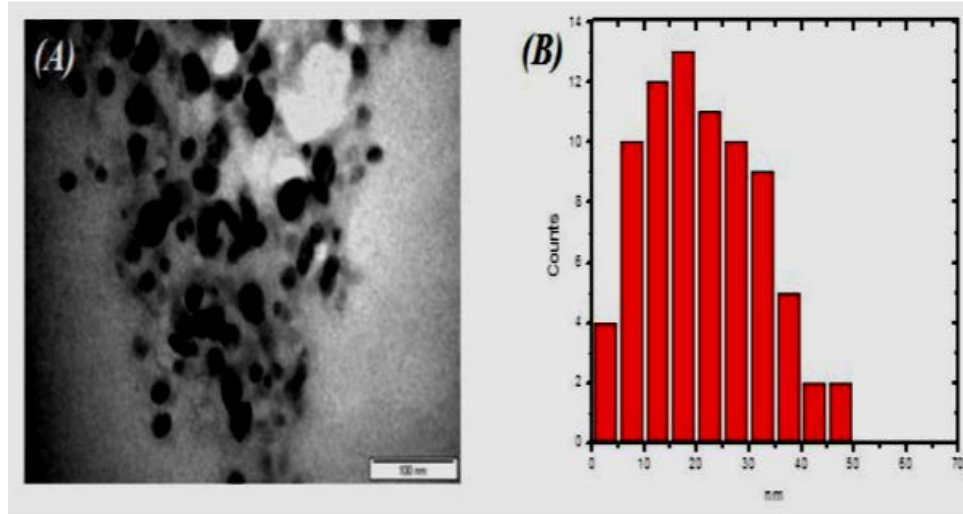


Figure 4: TEM image and size distribution histogram of the selenium nanoparticles produced by the reaction of 1 mM aqueous SeO_2 solution with bacteria *Providencia vermicola* BGRW culture at 37°C and pH 7.0 incubate for 24 h.

3.3.4. X-Ray Diffraction (XRD) analysis of selenium nanoparticles

X-ray diffraction is generally applied to a certain chemical arrangement and crystal design of an objective and it can be used for exposing the presence of SeNPs. The X-ray diffraction pattern obtained for the selenium nanoparticles that synthesized by *Providencia vermicola* BGRW is shown in Figure 5. Indexing process of powder diffraction pattern is done and Miller Indices (h k l) to each peak was assigned as shown in Figure 5, the XRD pattern exhibited identical diffraction peaks corresponding to the [(03), (065) and (1096) appearing at 65.8043°], [(01), (085) and (0567) appearing at 58.2°], [(00), (001) and (0848) appearing at 23.462°] and [(00), (027) and (0601) appearing at 28.3438° , 33.054° , 45.469° , 43.3599°] of metal selenium, indicates that the precipitate was composed of pure crystalline selenium. An overwhelmingly strong diffraction peaks located at 65.8043 is ascribed to the (03), (065) and (1096) facets of face-centered cubic metal selenium structures, while diffraction peaks of other facets are much strong facets of face-centered hexagonal metal selenium structures, few cubically shaped particles were also presence. These observations indicate that the produced selenium nanoparticles by bacteria *Providencia vermicola* BGRW are a mixture of different selenium phases. Nearly similar to results were obtained by [72] whereas, the diffraction peaks of hexagonal SeNPs were at $2\theta = 23.9, 30.0, 41.7, 44.0, 45.7, 52.0, 56.4, 62.2, 65.5$ and 68.4 were for the (100), (101), (110), (102), (111), (201), (003), (202), (210) and (211) reflections of the pure hexagonal phase of selenium crystals. Also, there were

many studies produced other nature of crystalline with other diffraction peaks whereas the crystalline nature of the selenium nanoballs was reported by [73] using X-ray diffraction shows broad diffraction peaks at lower angles, hence confirming the amorphous/nanocrystalline nature of the sample. However, the XRD analysis for the extracellular red elemental selenium indicated three intense peaks in the whole spectrum of 2θ values ranging from 5 to 80, the diffractions peak at 2θ value of 23.780, 29.797 and 43.878 can be indexed to the (100), (101) and (102) planes of the face-centered cubic (fcc) red elemental selenium, respectively [36, 74] .

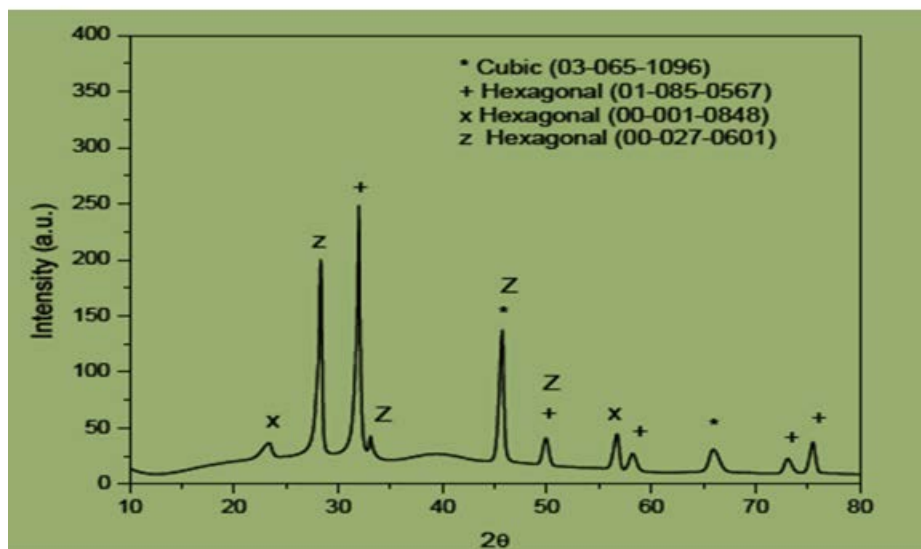


Figure 5: Representative XRD pattern of selenium nanoparticles synthesized by the reaction of BGRW culture with 1 mM SeO_2 solution at pH 7.0.

3.3.5. Fourier Transforms Infrared Spectroscopy (FTIR) analysis of selenium nanoparticles

Biosynthesized SeNPs that produced by BGRW were characterized by using (ATR-FTIR). The ATR-FTIR spectrum (Figure. 6) of bacterial crude protein and that bound to the SeNPs surface showed obvious changes in both the shape and the peak position suggesting the changes in the secondary structure of protein after nanoparticle formation. FTIR results revealed that secondary structure of proteins has been affected as a consequence of binding with SeNPs. ATR- FTIR spectra of SeNPs (Figure. 6) showed that several peaks appeared at 544, 618, 703, 1105, 1218, 1275, 1397, 1456, 1540, 1636, 3540, 3581, 3638, 3662 and 3774 cm^{-1} , are characteristic of proteins. The strong broad peaks at 3540, 3581, 3638, 3662 and 3774 cm^{-1} can be assigned to hydroxyl (OH) group and correspond to the amine group (NH stretching). The peak at 1456 and 1540 cm^{-1} are associated with CH stretching [75]. The bands at 1105 and 1397 cm^{-1} may be attributed to C-O stretching mode [76]. The peak at 703 cm^{-1} likely due to the presence of aromatic compounds [77]. Furthermore, the FTIR spectrum revealed two bands at 1636 and 1540 cm^{-1} corresponding to the amide I and II bands of proteins, respectively. The Amide I band is primarily a C=O stretching mode and the Amide II band is a combination of N-H in-plane bending and C-N stretching. The more complex Amide III band is located near 1397 cm^{-1} . The amide groups indicating the presence of enzymes were responsible for the reduction synthesis and stabilization of the metal ions [78]. This result indicates that molecules with these functional groups are associated with the NPs [79]. With the overall observations, it can be concluded that the proteins might have formed a capping

agent over the SeNPs, which may response for their stabilization [30]. Therefore, the produced SeNPs persisted for some months in liquid suspension. The peak at 618 cm^{-1} correspond to C–S sulfide stretching vibration, similarly the peak at 544 cm^{-1} showed S–S (polysulfide) stretching vibration indicating the frequent appearance of thiols and its substituted compounds constituting the backbone of the interacting protein. From the ATR-FTIR spectra, an interaction between SeNPs and protein is further confirmed by the shift in CH (1556 cm^{-1} to 1456 cm^{-1}), CN (1634 cm^{-1} to 1636 cm^{-1}), nitro compound (1401 cm^{-1} to 1397 cm^{-1}), aromatic compound (626 cm^{-1} to 618 cm^{-1}) and OH (3640 cm^{-1} to 3638 cm^{-1}). It is well known that free amine groups or cysteine residues the protein can bind to selenium nanoparticles that lead to the stabilization of SeNPs by surface-bound protein is a possibility were acting as natural capping agents, preventing agglomeration and promising medical activity. It is, therefore, inferable that the bio-reduction property of *Providencia vermicola* BGRW refer to its protein. Notably, the interaction between Se nanoparticles and protein is simply electrostatic between Se atoms and the NH, C=O groups [80]. In particular, Lenz and co-workers [81] showed that selenium nanoparticles can be bounded with a variety of high-affinity proteins. In addition, proteins and other biomolecules such as polysaccharides and fatty acid may play a key role in controlling SeNPs size and morphology [82].

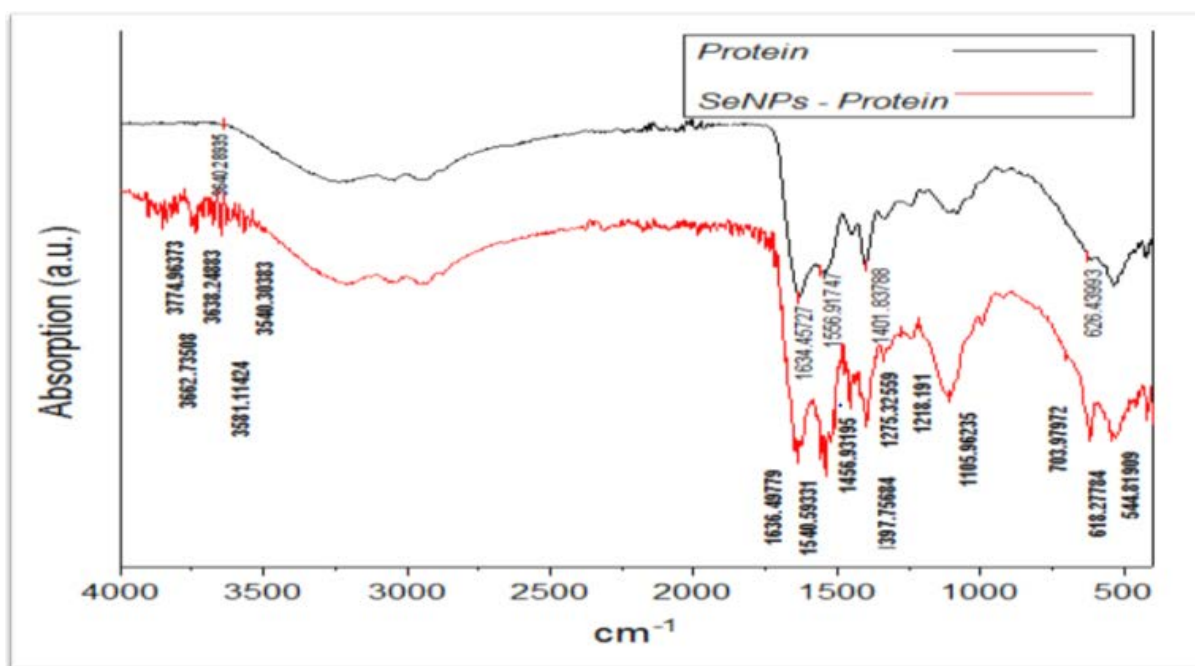


Figure 6: A representative ATR-FTIR spectrum pattern of dried powder of selenium nanoparticles synthesized by BGRW culture.

3.4. Antimicrobial activity of selenium nanoparticles

3.4.1. Determination of the inhibition zone of SeNPs at different concentrations

Different concentrations of biogenic SeNPs produced by *Providencia vermicola* BGRW were tested for their potential growth inhibition activity against various 14 pathogens by well diffusion method include these organisms *Staphylococcus aureus*, *Bacillus cereus*, *MRSA* (*Methicillin-resistant Staphylococcus aureus*),

Escherichia coli, *Pseudomonas aeruginosa*, *Enterobacter sp.*, *Enterococcus sp.*, *Proteus mirabilis*, *Klebsiella sp.*, *Streptococcus pneumoniae*, *Streptococcus agalactiae*, *Salmonella enteritidis*, *Candida albicans* and *Stenotrophomonas maltophilia*. Table 1 shows the diameter of the inhibition zone in mm of all pathogens. The highest antimicrobial activity of 100 µl SeNPs was seen in the order of *S. aureus* and *B. cereus* (29mm) (Figure. 7, B and D) followed by *MRSA* (27 mm) (Figure. 7, A), *S. agalactiae* (25 mm) and *E. coli* (13 mm) (Figure. 7, C). However, apart from *E. coli* SeNPs did not show a significant effect on the all bacterial growth of Gram-negative bacteria. The increases of SeNPs concentration lead to increase of diameter of inhibition zone, when the SeNPs concentrations were increased from 100µl (10µg) to 150µl (15µg), the diameter of inhibition zones were increased 14%, 17%, 24%, 31% and 37% against *S. aureus*, *B. cereus*, *S. agalactiae*, *E.coli* and *MRSA*, respectively. On the other hand, sub inhibitory concentration of SeNPs between 2.5-10 µg/mL had no antibacterial effect on tested strains [83]. However, sub-inhibitory concentration of SeNPs (2.5-10 µg/mL) were reported to have a stimulating effect on the growth of *Aspergillus niger* [39].

Table 1: Diameter of inhibition zone (mm) of different concentrations of SeNPs against various pathogens

Pathogens	SeNPs		Antibiotic					
	100 µl (10µg)	150 µl (15µg)	Gentamycin (GN) ¹⁰	Ampicillin (AMP) ²⁵	Norfloxacin (NX) ¹⁰	Sulfamethoxazole (SXT) ²⁵	Penicillin V (PNV) ¹⁰	Penicillin G (PNG) ¹⁰
<i>Staphylococcus aureus</i>	29	33	18	22	38	22	-	-
<i>Bacillus cereus</i>	29	34	21	31	43	33	-	8
<i>Streptococcus agalactiae</i>	25	31	26	21	21	28	-	-
<i>MRSA</i>	27	37	28	14	-	-	-	-
<i>Escherichia coli</i>	13	17	-	-	29	25	-	-

However, selenium nanoparticles have been reported to inhibit 95% of *S. aureus* and *E. coli* growth at high concentration (620µg/mL) (Alquthami, 2012). Tran and Webster [34] affirm that the SeNPs (chemically synthesized, with a range of 40-100 nm) showed inhibition effect against *S. aureus*. In the present study six antibiotics were used; sulfamethoxazole (SXT)²⁵, norfloxacin (NX)¹⁰, gentamicin (GN)¹⁰, ampicillin (AMP)²⁵, penicillin V (PNV)¹⁰ and penicillin G (PNG)¹⁰, to compare their inhibitory activity when combined with SeNPs against pathogenic bacteria which the SeNPs largest inhibition zone (29mm) of *S. aureus*, the largest zone was for sulfamethoxazole (22mm) followed by ampicillin (22mm), gentamicin (18mm), penicillin G (0 mm) and penicillin V (0 mm). While the SeNPs inhibition zone against *MRSA* was (27mm), the highest of all antibiotics which were used except gentamicin (28mm). The SeNPs inhibition zone against *B. cereus* was (29mm), the highest of gentamicin (21mm), penicillin G (8 mm) and penicillin V (0 mm). At *S. agalactiae*, the SeNPs inhibition zone was the highest of norfloxacin (21mm), ampicillin (21mm), penicillin G (0 mm) and penicillin V (0 mm). At last, SeNPs inhibition zone against *E. coli* (13mm) was an effective contrast of gentamicin,

ampicillin and penicillin which was resistant to them. (Table.1). Little information about the inhibition effect of SeNPs on the bacteria is available. From our results, biogenic SeNPs, therefore, appears to be reliable candidates for safe medical applications, to inhibit the growth of clinical isolates of *B. cereus*, *MRSA*, *S. aureus*, *S. agalactiae* and *E.coli*. However, in the present study, the biosynthesized SeNPs at concentrations of 10 µg displayed strong effect on the growth of all Gram- positive tested bacteria, including *S. aureus*, *B. cereus*, *MRSA* and *S. agalactiae*, in addition to a moderate effect on *E. coli* from Gram-negative bacteria.

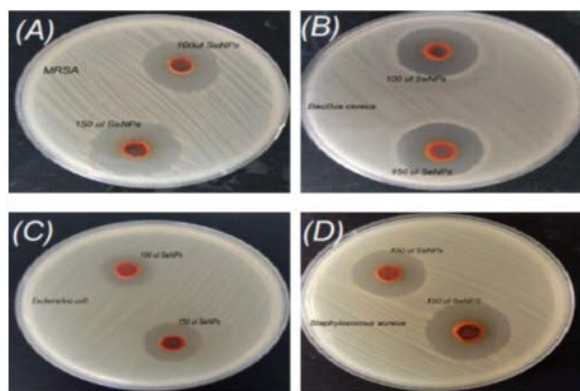


Figure 7: Antibacterial activity of different concentrations 100µl (10µg) and 150µl (15µg) of SeNPs against *MRSA* (A), *Bacillus cereus* (B), *Escherichia coli* (C) and *Staphylococcus aureus* (D).

3.4.2. Synergistic effect of SeNPs with antibiotic on antibacterial activity

The combination of selenium nanoparticles (SeNPs) and an antibiotic can synergistically inhibit bacterial pathogenic bacteria such as *E. coli*, *S. aureus*, *B. cereus*, *MRSA* and *S. agalactiae*. However, the mechanism for the synergistic activity is not known. This study chooses six of antibiotics: penicillin V (PNV), sulfamethoxazole (SXT), norfloxacin (NX), gentamicin (GN), ampicillin (AMP) and penicillin G (PNG) to explore their synergistic mechanism when combined with SeNPs against pathogenic bacteria. The combination of SeNPs with different antibiotics was investigated against five pathogenic bacteria using the disc diffusion method. The diameter of the inhibition zone in mm around the different antibiotic disks with and without SeNPs was determined as shown in (Table.2). The highest increase in fold area was found for Penicillin G in presence of SeNPs against *B. cereus* (387.5%), followed by *E. coli*, *S. aureus*, *MRSA* and *S. agalactiae* (100%). Likewise, for penicillin V, the increase fold areas were (100%) against all pathogens (Figure. 8, H). Similar for ampicillin, the increase fold area was (61%), whereas highest fold area observed against *E. coli* (100%), followed by *S. aureus* (90.9%), *MRSA* (71.4%) at (Fig.8, G), *S. agalactiae* (24%) and *B. cereus* (18.8%) (Figure. 8, I). The increase in fold area was also found the maximum for sulfamethoxazole combined with SeNPs against *MRSA* at (Figure. 8, F) and *E. coli* (100%), followed by *S. agalactiae* (14.3%) (Figure. 8, A) and *B. cereus* (8.6%). gentamicin was also enhanced by SeNPs and the highest increase in fold area was found against *E. coli* (100%), followed by *S. agalactiae* (30.7%) (Figure. 8, D), *B. cereus* (23.8%) (Figure. 8, C), *MRSA* (21.4%) (Figure. 8, E) and *S. aureus* (11.1%). At last, the highest increase in fold area of norfloxacin antibiotic was found against *E. coli* (13.8%), followed by *MRSA* (11.1%), *B. cereus* (9.3%) (Figure. 8, B) and *S. aureus* (5.3%). It indicated that the combination of antibiotics and selenium nanoparticles could increase the antibiotic efficacy against resistant

pathogens. However, the greatest enhancement was noticed with penicillin G (157.5%) and penicillin V (100%), followed by ampicillin (61%), sulfamethoxazole (44.6%), gentamicin (37.4%) and norfloxacin (7.9%). The enhancement of antibacterial activity could be due to the antibiotic-nanoparticle combination and not to the effect of NPs itself. It was found that the nanoparticles enhanced the reaction rates of antibiotics in a synergistic mode as well as in its own way on different kinds of pathogens [84]. The probable mechanism responsible in enhanced antibacterial activity of antibiotics with selenium nanoparticles may be attributed to the bonding reaction between nanoparticles and antibiotics, then the antibiotic-selenium nanoparticle combination may attach on the cell membrane result in cell wall lysis, which was followed by the entry of SeNPs-antibiotic combination into the cell and may result in the DNA unwinding leads to cell death, the same mechanism suggested by [85] about bonding reaction between silver nanoparticles and antibiotics. It is worth mentioning that this is the first report about the combination of selenium nanoparticles and various antibiotics against *S. aureus*, *MRSA*, *B. cereus*, *S. agalactiae* and *E.coli*. Recently, [86] showed successfully designed highly stable antibacterial SeNPs agents (quercetin – acetylcholine-SeNPs), this complex showed efficient antibacterial and bactericidal activities against superbugs. Due to the presence of acetylcholine, whereas this complex shows the ability to combine with the acetylcholine receptor on the bacterial cell membrane and increase the permeability of cell membranes. This causes membrane disruption and leads to the leakage of the cytoplasm, allowing nanocomposites to subsequently invade bacterial cells and disrupt DNA structure.

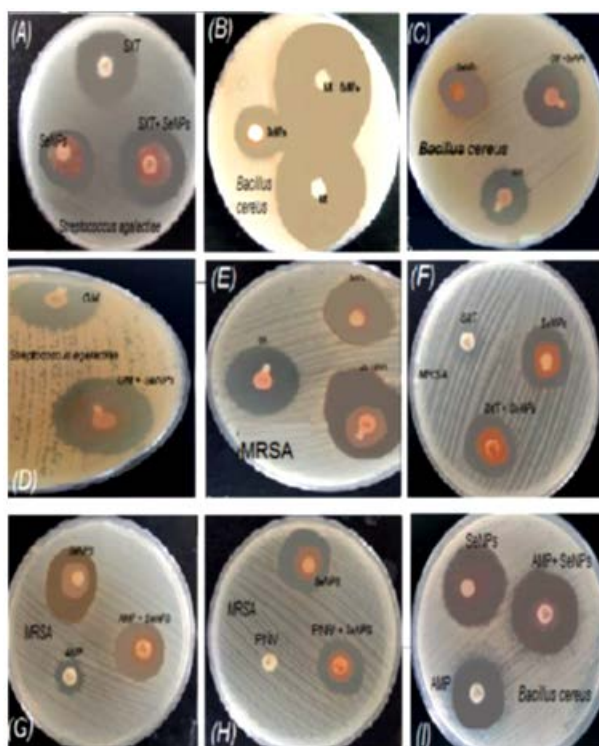


Figure 8: Digital Photograph of antibacterial activity of different antibiotic alone, selenium nanoparticles (SeNPs) and the combination of antibiotic with SeNPs against different pathogenic bacteria: (A&D) *S. agalactiae*, (B, C & I) *B. cereus* and (E, F, G & H) *MRSA*. The abbreviations: SXT= Sulfamethoxazole, NX= Norfloxacin, GM= Gentamicin, AMP= Ampicillin and PNV= Penicillin V.

Table 2: Diameter of inhibition zone (mm) of synergistic effect of SeNPs with various antibiotics

Diameter of inhibition zone																			
Pathogens	Norfloxacin (NX) ¹⁰				Ampicillin(AMP) ²⁵			Sulfamethoxazole(SXT) ²⁵			Penicillin V(PNV) ¹⁰			Penicillin G(PNG) ¹⁰			Gentamycin(GN) ¹⁰		
	SeNPs	NX	NX+ SeNPs	Fold area increasing	Amp	AMP+ SeNPs	Fold area increasing	SXT	SXT+SeNPs	Fold area increasing	PNV	PNV + SeNPs	Fold area increasing	PNG	PNG+ SeNPs	Fold area	GN	GN + SeNPs	Fold area increasing
Gram positive																			
<i>Staphylococcus aureus</i>	29	38	40	5.3%	22	42	90.9 %	32	32	0%	-	23	100%	-	41	100%	18	20	11.1 %
<i>Bacillus cereus</i>	29	43	47	9.3%	32	38	18.8 %	35	38	8.6%	-	25	100%	8	39	38.7 %	21	26	23.8 %
<i>Streptococcus agalactiae</i>	25	21	21	0%	25	31	24%	28	32	14.3%	-	23	100%	-	25	100%	26	34	30.7 %
<i>MRSA</i>	27	27	30	11.1%	14	24	71.4 %	-	18	100%	-	21	100%	-	23	100%	28	34	21.4 %
Gram negative																			

<i>Escherichia coli</i>	13	29	33	1 3. 8 %	-	7	100 %	-	14	100 %	-	15	100%	-	12	1 0 0 %	-	10	100%	
Overall synergistic antibacterial effect	7.9%		61%		44.6%		100%		157.5%		37.4%									

3.4.3. Determination the minimum inhibition concentration (MIC 90) of SeNPs

SeNPs were added to Luria-Bertani (LB) medium to reach predesigned concentrations whereas each pathogen strain was exposed to 5, 10, 15, 20 or 25 µg/mL of SeNPs. After a day of incubation, 1ml of a medium was sampled, diluted and then cultured on Luria-Bertani (LB) agar plates. OD600 was also monitored for different concentrations of SeNPs with a treated pathogen, considering the OD600 value of SeNPs in Luria-Bertani (LB) medium as background, it was expected that we could estimate bacterial numbers and obtain MIC (Minimum inhibition concentration) value by subtracting background from each measurement. It was found that there was no OD600 additive relationship between SeNPs and bacteria. After SeNPs were added to the bacterial culture, bacterial cells attracted SeNPs. Thus, the OD600 reading that would normally be generated by this portion of SeNPs was absent. As a result, to determine bacterial numbers with little influence from the SeNPs, CFU by plate counting was likely to be the only accurate method, CFU data were converted to bacterial numbers per ml, this result compatible with [87] result. OD600 was also monitored for different concentrations of SeNPs with a treated pathogen, considering the OD600 value of SeNPs in Luria-Bertani (LB) medium as background, it was expected that we could estimate bacterial numbers and obtain MIC (Minimum inhibition concentration) value by subtracting background from each measurement. It was found that there was no OD600 additive relationship between SeNPs and bacteria. After SeNPs were added to the bacterial culture, bacterial cells attracted SeNPs. Thus, the OD600 reading that would normally be generated by this portion of SeNPs was absent. As a result, to determine bacterial numbers with little influence from the SeNPs, CFU by plate counting was likely to be the only accurate method, CFU data were converted to bacterial numbers per ml, this result compatible with [87] result. The presence of SeNPs clearly showed reducing the bacterial numbers, high concentrations of SeNPs have more of an inhibitory effect on *S. aureus*, *B. cereus* and *E. coli* bacterial growth as compared to low concentrations (Figure. 9).

Minimum inhibition concentration of 90 % from bacterial growth (MIC 90) of *S.aureus*, *B. cereus* and *E. coli* were investigated, the MIC 90 of *S. aureus* was at 10µg/mL of SeNPs and at 15µg/mL of *B. cereus*, while the MIC 90 of *E. coli* was at 20µg/mL of SeNPs. Gram-positive bacteria were found to be far more sensitive to lower concentrations of SeNPs compared to Gram-negative bacteria. After 24 h at *S. aureus*, a concentration of 5µg/mL reduced cell populations by about 78% compared to control groups with no nanoparticles, high concentrations of nanoparticles (10µg/mL, 15µg/mL, 20µg/mL and 25µg/mL) also increased the number of dead cells as follow: 96%, 97%, 98% and 99%, respectively. Antibacterial activity was again attributed to increased oxidative stress and bacteria membrane interference. At *B. cereus*, a concentration of 5µg/mL reduced cell populations by about 62% compared to control groups with no nanoparticles, high concentrations of nanoparticles (10µg/mL, 15µg/mL, 20µg/mL and 25µg/mL) also increased the number of dead cells as follow: 80%, 98%, 99% and 100%, respectively. At 25µg/mL, no growth of *B. cereus* was found that mean, this concentration was microbial bactericidal concentration (MBC) as shown in (Figure. 9), the strong antibacterial activities were observed at all SeNPs concentrations against *B. cereus*.

At *E. coli*, a concentration of 5µg/mL reduced cell populations by about 12% compared to control groups with no nanoparticles, high concentrations of nanoparticles (10µg/mL, 15µg/mL, 20µg/mL and 25µg/mL) also increased the number of dead cells as follow: 26%, 78%, 92% and 99%, respectively. These results confirmed that the Gram-positive bacteria were more sensitive to SeNPs compared to gram-negative bacteria. We used 25 µg/ml sulfamethoxazole antibiotics as a control to compare the inhibition effect of SeNPs with it and the inhibition effects of *S.aureus*, *B. cereus* and *E. coli* were as follow: 95%, 96% and 98%, respectively as shown in (Figure. 9).

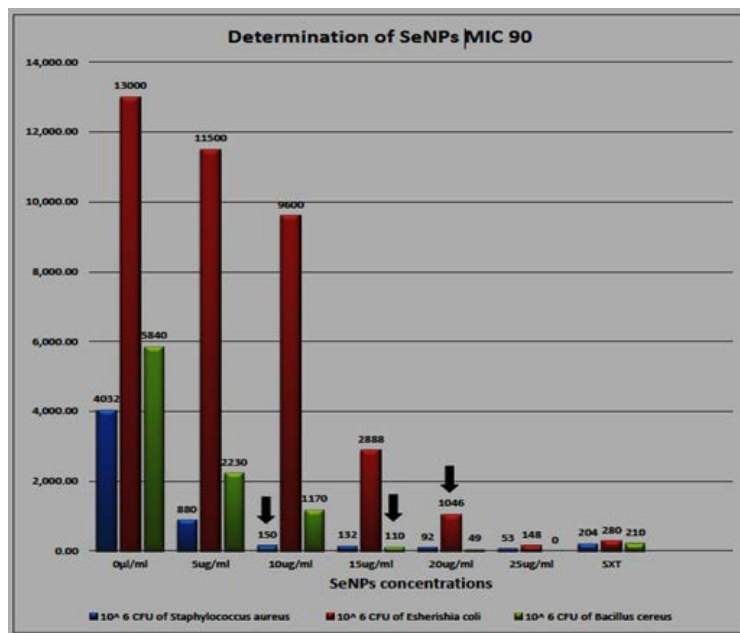


Figure 9: The diagram shows the antimicrobial effect of SeNPs against three pathogens with different concentrations 0µg/mL, 10µg/mL, 15µg/mL, 20µg/mL and 25µg/mL to determine MIC 90, the growth of the tested strains was measured as CFU by plate counting method.

3.4.4. Scanning electron microscopy (SEM) to pathogens treated with selenium nanoparticles

Additionally, images obtained using scanning electron microscope (SEM) helped in a detailed investigation of the topological changes in bacterial shape. Upon interaction with SeNPs, the bacterial membrane surface potential was weakened and neutralized, resulting in increase in surface tension. At high concentration of SeNPs, the interactions result in surface tension change which leads to the membrane depolarization at the point of contact. As a result, bacterial membrane show abnormal textures like membrane rupture, membrane blebs, the ruptured cells often found in aggregates or clumps (Figures. 10, 11 and 12). Morphology and structure of Gram-positive strain *S. aureus* treated with SeNPs (Figure. 10, B) and untreated cells (Figure. 10, A) were observed using SEM imaging in order to study the mechanisms of the antibacterial interactions. The following concentration was selected because they display strong antibacterial effects: 25 µg/mL SeNPs, samples were withdrawn and fixed for 6 h. Untreated cells were typically cocci-shape bacteria whereas, treated cells with SeNPs showed damage to the cell wall and clumps of cells. In *B. cereus* cells, untreated cells (Figure. 11, A) were typically rod-shaped bacteria whereas, treated cells with SeNPs (Figure. 11, B) for 6 h showed damage to cell wall and aggregates of bacterial cells.

Morphology and structure of *Escherichia coli* as gram-negative bacteria, untreated and treated cells with SeNPs were observed, untreated cells were typically rod-shaped bacteria (Figure. 12, A) whereas, treated cells with SeNPs (Figure. 12, B) clearly showed membrane rupture, membrane blebs, clumps cells. These results are in parallel with the results obtained by [88].

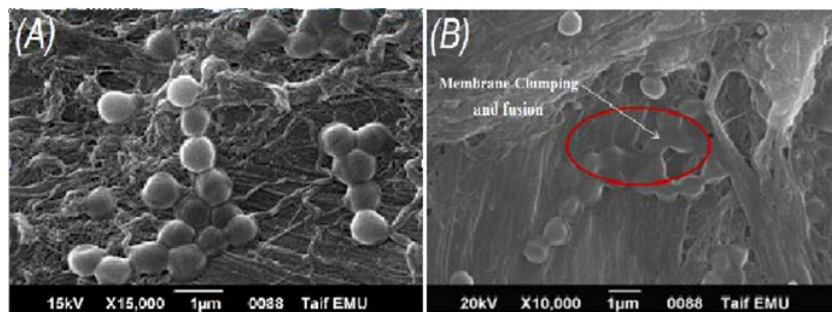


Figure 10: Visualization of SeNPs treated *S. aureus* cells surface by SEM, (A) control (without NPs treated cells) and (B) showing membrane clumping and fusion in SeNPs treated cells.

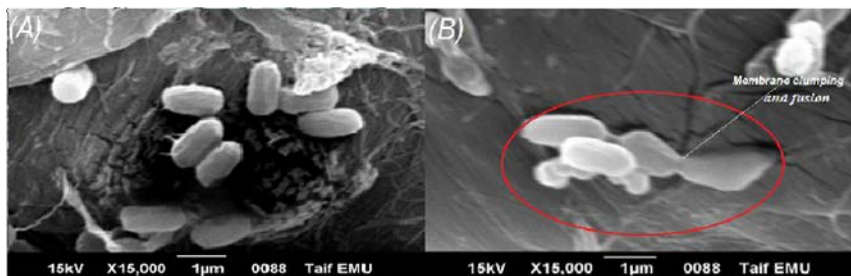


Figure 11: Visualization of SeNPs treated *B. cereus* cell surface by SEM, (A) control (without NPs treated cells) and (B) showing membrane clumping and fusion in SeNPs treated cells.

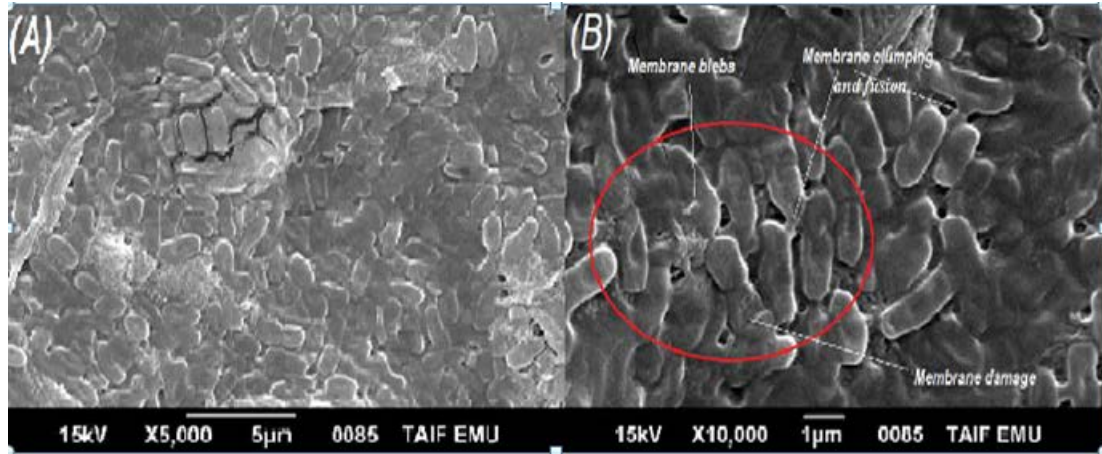


Figure 12: Visualization of SeNPs treated *E. coli* cell surface by SEM, (A) control (without NPs treated cells) and (B) showing membrane damaging, clumping, fusion and blebs in SeNPs treated cells.

3.4.5. The antibiofilm effect of the SeNPs

According to the report of the National Institutes of Health and Center of Disease control, about ~65–80 % infections occurred by biofilm forming microbes [89]. The antibiofilm effect of the SeNPs against different pathogens which have ability to establish biofilms; the Gram-positive tested pathogens were (*S. aureus* and *B. cereus*) and the Gram-negative tested pathogens were (*E. coli*, *Proteus sp.*, *Pseudomonas aeruginosa* and *Salmonella enteritidis*) were investigated in vitro using polystyrene microtiter plate technique (Table.3). In the absence of SeNPs, all strains were strong biofilm producers (+++).

The biofilm forming ability of all tested strains changed from to incorporate 4µg/mL of SeNPs in the incubation medium. Remarkably, all strains became moderate biofilm producers (++) in presence of 4µg/mL of SeNPs. By increasing the SeNPs concentration to 8µg/mL, *E.coli*, *Sal. enteritidis* and *S. aureus* changed to be weak biofilm producers (+), while *B. cereus*, *Proteus sp.* and *P. aeruginosa* remained in the categories of moderate biofilm. The obtained results demonstrated that the antibiofilm concentration of SeNPs against *Sal. enteritidis* and *B. cereus* was 12µg/mL, the antibiofilm concentration of SeNPs against *S. aureus* and *E. coli* was 16µg/mL, while the antibiofilm concentration of SeNPs against *Proteus sp.* and *P. aeruginosa* was 18µg/mL. SeNPs showed a significant antibiofilm effect of Gram-negative and Gram-negative bacteria. The increases of SeNPs concentration lead to increase of inhibition effect of biofilm formation, the biofilm inhibition effects increased 67%, 80%, 88% and 97% against *S. aureus*, when SeNPs concentrations were 4, 8, 12 and 16µg/mL, respectively. The biofilm inhibition effects increased 13%, 31%, 93% and 97% against *B. cereus*, when SeNPs concentrations were 4, 8, 12 and 16µg/mL, respectively.

The biofilm inhibition effects against Gram-negative bacteria increased 28%, 70%, 71%, 97% and 100% against *E. coli*, when SeNPs concentrations were 4, 8, 12, 16 and 18µg/mL, respectively. While the biofilm inhibition effects of *Proteus sp.* increased 31%, 49%, 53%, 66% and 78%, when SeNPs concentrations were 4, 8, 12, 16 and 18µg/mL, respectively. However, *P. aeruginosa* lost 60%, 64%, 70%, 75% and 86% but *Sal. enteritidis* lost 58%, 64%, 88%, 93% and 97% of their ability to biofilm formation, when SeNPs concentrations were 4, 8, 12,

16 and 18µg/mL, respectively. The first study on the antibiofilm effect of SeNPs (with the particle-size range of 80-220 nm) against *S. aureus*, *P. aeruginosa*, and *P. mirabilis* was carried out by [64].

The SeNPs (with particle-size average 28 nm) produced in the present study has sharp effect as an antibiofilm agent against *S. aureus*, *B. cereus*, *E. coli* and *Sal. enteritidis* where they lost their ability to form biofilm above (95%). At recent study, the SeNPs were able to inhibit biofilm formation and also to disaggregate the mature glycocalyx in both *P. aeruginosa* and *Candida sp.* and reported that the biogenic SeNPs achieved much stronger antibiofilm effects than chemically synthetic selenium nanoparticles [90].

3.4.6. The ability of SeNPs to remove the established biofilm

The effect of SeNPs on removing the established biofilm (after 24 h) was studied in microtiter plates against the studied pathogens which had the ability to establish biofilms; the Gram-positive tested pathogens were (*S. aureus*, *B. cereus*) and the Gram-negative tested pathogens were (*E. coli*, *Proteus sp.*, *P. aeruginosa* and *Sal. enteritidis*) were investigated in vitro. Different SeNPs concentrations from 20 (the antibiofilm concentration) up to 32 µg/mL were added during washing steps (Table.4). Washing with PBS containing SeNPs up to 20µg/mL showed a slight effect as a removing agent against the established biofilm developed by all tested strains whereas the strong biofilm turned to moderate biofilm except *E.coli* whereas, at 24µg/mL, the established biofilm was moderate. Incorporation of 32µg/mL of SeNPs showed a stronger effect in removing agent against all studied bacteria whereas all established biofilm became weak biofilms. SeNPs are known to have killing effect against *S. aureus* [34]. This could provide an interpretation for the slight removing effect of SeNPs obtained in the present study, where the dead cells could lose their ability to adhere to the surviving cells in the polysaccharide matrix of the established biofilm resulting in the dispersal of a subpopulation of surviving cells [91].

The obtained results indicated that the SeNPs produced by *Providencia vermicola* BGRW under the studied conditions had slight ability to remove established biofilm of different bacteria. In another study [92] reported that SeNPs completely eradicated the biofilm structure of *E. coli* at a concentration of 60µg/L. At the same concentration, SeNPs destroyed most part of biofilms cells of both *P. aeruginosa* and *S. aureus*, in contrast to growth control, formed for the most part of viable cells. At this point, the last study by [90] resulted that the *P. aeruginosa* biofilm was highly susceptible to SeNPs induced disaggregation, resulting in 0% degradation in the presence of 50 µg/ml SeNPs, confirming that this strain is more susceptible to SeNPs than the other strains.

The exposure of the other *P. aeruginosa* 50–100 µg/ml SeNPs resulted in 50–70% biofilm dissolution and this did not increase at higher SeNPs concentrations. The biogenic SeNPs eliminated 45–60% of the yeast biofilms at the lowest SeNPs doses (50–100 µg/ml) and there was no improvement at higher doses.

According to results, selenium nanoparticles did not have the ability to detach elute the entire established biofilms of *S. aureus*, *B. cereus*, *E. coli*, *Proteus sp.*, *P. aeruginosa* and *Sal. enteritidis*, at high concentrations and just changed them to weak biofilms.

Table 3: Antibiofilm effect of the biosynthesized selenium nanoparticles (SeNPs) against some pathogens

Pathogens		SeNPs concentration (µg/ml)						
		0	4	8	12	16	18	NC
Gram positive								
<i>Staphylococcus aureus</i>	OD ₅₇₀	0.985	0.321	0.199	0.118	0.02	0.05	0.116
	Strong of biofilm	+++	++	+	+	-	-	
	Percent of inhibition		67%	80%	88%	97%	95%	
<i>Bacillus cereus</i>	OD ₅₇₀	0.450	0.390	0.310	0.033	0.015	0.02	0.105
	Strong of biofilm	+++	++	++	-	-	-	
	Percent of inhibition		13%	31%	93%	97%	95%	
Gram negative								
<i>Escherichia coli</i>	OD ₅₇₀	0.532	0.382	0.162	0.154	0.015	0.00	0.116
	Strong of biofilm	+++	++	+	+	-	-	
	Percent of inhibition		28%	70%	71%	97%	100%	
<i>Proteus sp.</i>	OD ₅₇₀	1.301	0.897	0.658	0.608	0.446	0.25	0.27
	Strong of biofilm	+++	++	++	++	+	-	
	Percent of inhibition		31%	49%	53%	66%	78%	
<i>Pseudomonas aeruginosa</i>	OD ₅₇₀	1.503	0.602	0.541	0.450	0.38	0.203	0.27
	Strong of biofilm	+++	++	++	+	+	-	
	Percent of inhibition		60%	64%	70%	75%	86%	
<i>Salmonella enteritidis</i>	OD ₅₇₀	0.603	0.249	0.22	0.067	0.045	0.018	0.105
	Strong of biofilm	+++	++	+	-	-	-	
	Percent of inhibition		58%	64%	88%	93%	97%	

(NC) negative control; (-) No; (+) weak; (++) moderate; (+++) strong biofilm producer

3.4.7. Synergistic effect of SeNPs combination with antibiotic on antibiofilm activity

The combination of selenium nanoparticles (SeNPs) and an antibiotic may synergistically inhibit biofilm

formation of pathogenic bacteria such as *S. aureus*, *B. cereus*, *E. coli*, *Proteus sp.*, *P. aeruginosa* and *Sal. enteritidis*. In this study amoxicillin (AMC) was chosen to explore synergistic effect when combined with SeNPs against bacterial biofilm formation. The combination of SeNPs with antibiotic was investigated against six bacterial biofilms using the polystyrene microtiter plate technique (Table.5). In the absence of SeNPs and Amoxicillin, all strains were strong biofilm producers (+++).

The biofilm inhibition effect was analyzed in presence of different concentrations (7.5, 10, 12.5, 15, 17.5, 20 and 25µg/ml) of SeNPs with the same concentrations (7.5, 10, 12.5, 15, 17.5, 20 and 25µg/ml) of AMC that means we used (15, 20, 25, 30, 35, 40 and 50µg/ml) concentrations of 1(SeNPs):1(AMC)

First, the effect of amoxicillin on biofilm forming ability was determined to comparing this antibiofilm activity with the synergistic activity of the combination of SeNPs and amoxicillin (Table.5). The biofilm forming ability of all tested strains changed after the incorporation of 15µg/mL AMC in the incubation medium. Remarkably, all strains became moderate biofilm producers (++) as a result of treatment with 15µg/mL AMC except *Sal. enteritidis* which became weak biofilm-producers (+). The obtained results demonstrated that the antibiofilm concentration of AMC against *Sal. enteritidis* and *Proteus sp.* was 25µg/mL, the antibiofilm concentration of AMC against *S. aureus*, *E. coli*, *Proteus sp.* and *P. aeruginosa* did not appear even to 50µg/mL. AMC did not show a significant antibiofilm effect of *S. aureus*, *E. coli*, *Proteus sp.* and *P. aeruginosa*. By increasing the AMC concentration to 35µg/mL, *S. aureus*, *Proteus sp.* and *P. aeruginosa* changed to be weak biofilm-producer (+) while *E. coli* still in the categories of moderate biofilm and change to weak biofilm at 40µg/mL. Biofilm formation was not significantly reduced in the case of antibiotic alone. The biofilm forming ability of all tested strains changed clearly when the combination of selenium nanoparticles and amoxicillin were used (Table.5). The biofilm forming ability changed from to incorporate 15µg/mL (7.5µg/mL of AMC and 7.5µg/mL of SeNPs). Remarkably, *S. aureus* and *E.coli* strains did not produce biofilms (-) that means the antibiofilm effect was synergistically inhibited by added (7.5µg/mL of AMC and 7.5µg/mL of SeNPs) comparing to high concentration of AMC which need to changed *S. aureus* and *E.coli* biofilms just to weak biofilm procedure, meanwhile *B. cereus* , *Sal. enteritidis* and *Proteus sp.* strains became no biofilm-producers as a result of treatment with 20µg/mL(10µg/mL of AMC and 10µg/mL of SeNPs) but the antibiofilm concentration at *P. aeruginosa* was 25µg/mL(12.5µg/mL of AMC and 12.5µg/mL of SeNPs). The previous results about the antibiofilm concentration of SeNPs against *Sal. enteritidis* and *B. cereus* was 12µg/mL, the antibiofilm concentration of SeNPs against *S. aureus* and *E. coli* was 16µg/mL, while the antibiofilm concentration of SeNPs against *Proteus sp.* and *P. aeruginosa* was 18µg/mL, these antibiofilm concentrations of SeNPs without any addition confirm to us that the antibiofilm effect of SeNPs and AMC did not a result of the effect each one of them individually. The enhancement of antibiofilm activity could be due to the antibiotic-nanoparticle combination and not to the effect of NPs itself. These are encouraging results, as it may be possible to achieve an effective anti-biofilm effect at lower antibiotic concentrations. Therefore, SeNPs and their combination with antibiotic could be used as an anti-biofilm agent against bacterial biofilms. At similar study on another type of nanoparticles [93] reported that combinations of Ag-NPs and antibiotics led to an increase in inhibitory effect on biofilm formation with different degrees, yet, generally showed a greater inhibitory activity than AgNPs or antibiotic alone.

Table 4: Biofilm removing ability of the biosynthesized SeNPs against some pathogens

Pathogens		SeNPs concentration (µg/ml)					
		0	20	24	28	32	NC
Gram positive							
<i>Staphylococcus aureus</i>	OD ₅₇₀	0.985	0.370	0.358	0.306	0.457	0.24
	Strong of biofilm	+++	++	+	+	+	
<i>Bacillus cereus</i>	OD ₅₇₀	0.592	0.327	0.297	0.232	0.244	0.13
	Strong of biofilm	+++	++	++	+	+	
Gram negative							
<i>Escherichia coli</i>	OD ₅₇₀	0.653	0.571	0.362	0.319	0.260	0.126
	Strong of biofilm	+++	+++	++	++	+	
<i>Proteus sp.</i>	OD ₅₇₀	1.301	0.235	0.147	0.251	0.256	0.231
	Strong of biofilm	+++	++	++	++	+	
<i>Pseudomonas aeruginosa</i>	OD ₅₇₀	1.503	0.368	0.358	0.303	0.245	0.283
	Strong of biofilm	+++	++	++	+	+	
<i>Salmonella enteritidis</i>	OD ₅₇₀	0.603	0.390	0.350	0.329	0.265	0.165
	Strong of biofilm	+++	++	++	+	+	

4. Conclusion

In the present, all tested antibiotics showed synergistic inhibition against the growth of the pathogenic bacteria. The TEM images showed damage in the cell wall of the tested microbes resulting the death of cells. The MIC 90 of SeNPs was 10µg/mL, 15µg/mL and 20µg/mL for *S. aureus*, *B. cereus* and *E. coli* respectively. The antibiofilm concentration of SeNPs was 12µg/mL against *Sal. enteritidis* and *B. cereus*, 16µg/mL against *S. aureus* and *E. coli* while the antibiofilm concentration was 18µg/mL against *Proteus sp.* and *P. aeruginosa*. The concentration of 24µg/mL showed a slight effect on removing the established biofilm. The antibiofilm effect of the combination of SeNPs with amoxicillin showed a synergistic effect at a lower than the antibiotic or SeNPs minimum antibiofilm concentrations.

Table 5: OD₅₇₀ values of synergistic effect of the biosynthesized SeNPs with amoxicillin against some pathogens biofilm

Biofilm type	NC	PC	15µg/mL of AMC	20µg/mL of AMC +SeNPs	25µg/mL of AMC +SeNPs	30µg/mL of AMC +SeNPs	35µg/mL of AMC +SeNPs	40µg/mL of AMC +SeNPs	50µg/mL of AMC +SeNPs							
Gram positive																
<i>Staphylococcus aureus</i>	0.255	0.989 +++	0.548 ++	0.173 -	0.559 ++	0.156 -	0.583 ++	0.158 -	0.582 ++	0.132 -	0.439 +	0.143 -	0.437 +	0.201 -	0.423 +	0.198 -
<i>Bacillus cereus</i>	0.211	0.83 +++	0.460 ++	0.235 +	0.463 ++	0.186 -	0.474 ++	0.161 -	0.472 ++	0.162 -	0.435 +	0.131 -	0.358 +	0.144 -	0.236 +	0.201 -
Gram negative																
<i>Escherichia coli</i>	0.172	0.753 +++	0.534 ++	0.118 -	0.526 ++	0.129 -	0.523 ++	0.116 -	0.505 ++	0.128 -	0.388 ++	0.142 -	0.352 +	0.143 -	0.346 +	0.107 -
<i>Proteus sp.</i>	0.164	1.201 +++	0.387 ++	0.328 ++	0.246 +	0.152 -	0.143 -	0.142 -	0.138 -	0.160 -	0.158 -	0.123 -	0.099 -	0.098 -	0.143 -	0.112 -

	0.124	0.073
	-	-
	0.334	0.019
	+	-
	0.127	0.053
	-	-
	0.345	0.025
	+	-
	0.135	0.123
	-	-
	0.452	0.057
	+	-
	0.143	0.151
	-	-
	0.484	0.063
	++	-
	0.147	0.142
	-	-
	0.511	0.166
	++	-
	0.390	0.153
	+	-
	0.519	0.198
	++	+
	0.411	0.233
	+	+
	0.632	0.254
	++	+
	1.589	0.932
	+++	+++
	0.230	0.175
<i>Pseudomonas aeruginosa</i>		
<i>Salmonella enteritidis</i>		

(NC) negative control ;(PC) positive control; (-) No; (+) weak; (++) moderate; (+++) strong biofilm producer

References

- [1] W. Wang, D. Cheng, F. Gong, X. Miao, and X. Shuai, "Design of Multifunctional Micelle for Tumor-Targeted Intracellular Drug Release and Fluorescent Imaging," *Advanced Materials*, vol. 24, pp. 115-120, 2012.
- [2] U. K. Parashar, P. S. Saxena, and A. Srivastava, "Bioinspired synthesis of silver nanoparticles," *Digest Journal of Nanomaterials & Biostructures (DJNB)*, vol. 4, 2009.
- [3] P. Mohanpuria, N. K. Rana, and S. K. Yadav, "Biosynthesis of nanoparticles: technological concepts and future applications," *Journal of Nanoparticle Research*, vol. 10, pp. 507-517, 2008.
- [4] N. Krumov, I. Perner-Nochta, S. Oder, V. Gotcheva, A. Angelov, and C. Posten, "Production of inorganic nanoparticles by microorganisms," *Chemical engineering & technology*, vol. 32, pp. 1026-1035, 2009.
- [5] J. Y. Kim, F. E. Osterloh, H. Hiramatsu, R. Dumas, and K. Liu, "Synthesis and real-time magnetic manipulation of a biaxial superparamagnetic colloid," *The Journal of Physical Chemistry B*, vol. 109, pp. 11151-11157, 2005.
- [6] Z. Li and Y. Du, "Biomimic synthesis of CdS nanoparticles with enhanced luminescence," *Materials Letters*, vol. 57, pp. 2480-2484, 2003.
- [7] T. Schlorf, M. Meincke, E. Kossel, C.-C. Glüer, O. Jansen, and R. Mentlein, "Biological properties of iron oxide nanoparticles for cellular and molecular magnetic resonance imaging," *International journal of molecular sciences*, vol. 12, pp. 12-23, 2010.
- [8] F. M. Fordyce, *Selenium deficiency and toxicity in the environment*: Springer, 2013.
- [9] D. N. Cox and K. Bastiaans, "Understanding Australian consumers' perceptions of selenium and motivations to consume selenium enriched foods," *Food Quality and Preference*, vol. 18, pp. 66-76, 2007.
- [10] N. V. Ralston, C. R. Ralston, J. L. Blackwell, and L. J. Raymond, "Dietary and tissue selenium in relation to methylmercury toxicity," *Neurotoxicology*, vol. 29, pp. 802-811, 2008.
- [11] P. Craig and W. Maher, "10 Organoselenium Compounds in the Environment," *Organometallic Compounds in the Environment*, p. 391, 2003.
- [12] L. Wu, "Review of 15 years of research on ecotoxicology and remediation of land contaminated by agricultural drainage sediment rich in selenium," *Ecotoxicology and environmental safety*, vol. 57, pp. 257-269, 2004.

- [13] C. Ip, H. J. Thompson, Z. Zhu, and H. E. Ganther, "In vitro and in vivo studies of methylseleninic acid: evidence that a monomethylated selenium metabolite is critical for cancer chemoprevention," *Cancer research*, vol. 60, pp. 2882-2886, 2000.
- [14] S. MILLER, S. W. WALKER, J. R. ARTHUR, F. NICOL, K. PICKARD, M. H. LEWIN, et al., "Selenite protects human endothelial cells from oxidative damage and induces thioredoxin reductase," *Clinical science*, vol. 100, pp. 543-550, 2001.
- [15] B. Langi, C. Shah, K. Singh, A. Chaskar, M. Kumar, and P. N. Bajaj, "Ionic liquid-induced synthesis of selenium nanoparticles," *Materials Research Bulletin*, vol. 45, pp. 668-671, 2010.
- [16] K. N. Thakkar, S. S. Mhatre, and R. Y. Parikh, "Biological synthesis of metallic nanoparticles," *Nanomedicine: Nanotechnology, Biology and Medicine*, vol. 6, pp. 257-262, 2010.
- [17] S. Magdassi, M. Grouchko, and A. Kamyshny, "Copper nanoparticles for printed electronics: routes towards achieving oxidation stability," *Materials*, vol. 3, pp. 4626-4638, 2010.
- [18] J. W. Doran, "Microorganisms and the biological cycling of selenium," in *Advances in microbial ecology*, ed: Springer, 1982, pp. 1-32.
- [19] H. DeMoll-Decker and J. M. Macy, "The periplasmic nitrite reductase of *Thauera selenatis* may catalyze the reduction of selenite to elemental selenium," *Archives of microbiology*, vol. 160, pp. 241-247, 1993.
- [20] W. J. Hunter and L. D. Kuykendall, "Identification and characterization of an *Aeromonas salmonicida* (syn *Haemophilus piscium*) strain that reduces selenite to elemental red selenium," *Current microbiology*, vol. 52, pp. 305-309, 2006.
- [21] J. Kessi, "Enzymic systems proposed to be involved in the dissimilatory reduction of selenite in the purple non-sulfur bacteria *Rhodospirillum rubrum* and *Rhodobacter capsulatus*," *Microbiology*, vol. 152, pp. 731-743, 2006.
- [22] W. J. Hunter and L. D. Kuykendall, "Reduction of selenite to elemental red selenium by *Rhizobium* sp. strain B1," *Current microbiology*, vol. 55, pp. 344-349, 2007.
- [23] P. Antonioli, S. Lampis, I. Chesini, G. Vallini, S. Rinalducci, L. Zolla, et al., "*Stenotrophomonas maltophilia* SeITE02, a new bacterial strain suitable for bioremediation of selenite-contaminated environmental matrices," *Applied and environmental microbiology*, vol. 73, pp. 6854-6863, 2007.
- [24] W. J. Hunter and D. K. Manter, "Reduction of selenite to elemental red selenium by *Pseudomonas* sp. strain CA5," *Current microbiology*, vol. 58, pp. 493-498, 2009.
- [25] M. Bajaj, S. Schmidt, and J. Winter, "Formation of Se (0) Nanoparticles by *Duganella* sp. and

- Agrobacterium sp. isolated from Se-laden soil of North-East Punjab, India," *Microbial cell factories*, vol. 11, p. 1, 2012.
- [26] S. He, Z. Guo, Y. Zhang, S. Zhang, J. Wang, and N. Gu, "Biosynthesis of gold nanoparticles using the bacteria *Rhodospseudomonas capsulata*," *Materials Letters*, vol. 61, pp. 3984-3987, 2007.
- [27] M. Gericke and A. Pinches, "Microbial production of gold nanoparticles," *Gold bulletin*, vol. 39, pp. 22-28, 2006.
- [28] Y. Nangia, N. Wangoo, N. Goyal, G. Shekhawat, and C. R. Suri, "Microbial cell factories Volume: 8 ISSN: 1475-2859 ISO Abbreviation: Microb. Cell Fact. Publication Date: 2009," Detail:.
- [29] K. B. Narayanan and N. Sakthivel, "Biological synthesis of metal nanoparticles by microbes," *Advances in colloid and interface science*, vol. 156, pp. 1-13, 2010.
- [30] P. Sonkusre, R. Nanduri, P. Gupta, and S. S. Cameotra, "Improved extraction of intracellular biogenic selenium nanoparticles and their specificity for cancer chemoprevention," *Journal of Nanomedicine & Nanotechnology*, vol. 2014, 2014.
- [31] S. Lampis, E. Zonaro, C. Bertolini, P. Bernardi, C. S. Butler, and G. Vallini, "Delayed formation of zero-valent selenium nanoparticles by *Bacillus mycoides* SeITE01 as a consequence of selenite reduction under aerobic conditions," *Microbial cell factories*, vol. 13, p. 1, 2014.
- [32] G. M. Khiralla and B. A. El-Deeb, "Antimicrobial and antibiofilm effects of selenium nanoparticles on some foodborne pathogens," *LWT-Food Science and Technology*, vol. 63, pp. 1001-1007, 2015.
- [33] T. Mennini, "Elemental selenium nanoparticles with reduced toxicity," *Nutrafoods*, vol. 11, pp. N25-N26, 2012.
- [34] P. A. Tran and T. J. Webster, "Selenium nanoparticles inhibit *Staphylococcus aureus* growth," *Int J Nanomedicine*, vol. 6, pp. 1553-1558, 2011.
- [35] J. Yang, K. Huang, S. Qin, X. Wu, Z. Zhao, and F. Chen, "Antibacterial action of selenium-enriched probiotics against pathogenic *Escherichia coli*," *Digestive diseases and sciences*, vol. 54, pp. 246-254, 2009.
- [36] N. Singh, P. Saha, K. Rajkumar, and J. Abraham, "Biosynthesis of silver and selenium nanoparticles by *Bacillus* sp. JAPSK2 and evaluation of antimicrobial activity," *Der Pharm Lett*, vol. 6, pp. 175-181, 2014.
- [37] K. Alquthami, "Antibacterial effect of selenium, germanium, and lithium on clinically important bacteria growing in planktonic culture and biofilms: some medical implications," University of Sheffield, 2012.

- [38] E. Kheradmand, F. Rafii, M. H. Yazdi, A. A. Sepahi, A. R. Shahverdi, and M. R. Oveisi, "The antimicrobial effects of selenium nanoparticle-enriched probiotics and their fermented broth against *Candida albicans*," *DARU Journal of Pharmaceutical Sciences*, vol. 22, p. 48, 2014.
- [39] Z. B. Kazempour, M. H. Yazdi, F. Rafii, and A. R. Shahverdi, "Sub-inhibitory concentration of biogenic selenium nanoparticles lacks post antifungal effect for *Aspergillus niger* and *Candida albicans* and stimulates the growth of *Aspergillus niger*," *Iranian journal of microbiology*, vol. 5, p. 81, 2013.
- [40] S. Dhanjal and S. S. Cameotra, "Aerobic biogenesis of selenium nanospheres by *Bacillus cereus* isolated from coalmine soil," *Microbial cell factories*, vol. 9, p. 1, 2010.
- [41] P. J. Fesharaki, P. Nazari, M. Shakibaie, S. Rezaie, M. Banoe, M. Abdollahi, et al., "Biosynthesis of selenium nanoparticles using *Klebsiella pneumoniae* and their recovery by a simple sterilization process," *Brazilian Journal of Microbiology*, vol. 41, pp. 461-466, 2010.
- [42] R. Cui, H. H. Liu, H. Y. Xie, Z. L. Zhang, Y. R. Yang, D. W. Pang, et al., "Living yeast cells as a controllable biosynthesizer for fluorescent quantum dots," *Advanced Functional Materials*, vol. 19, pp. 2359-2364, 2009.
- [43] A. K. Suresh, "Extracellular bio-production and characterization of small monodispersed CdSe quantum dot nanocrystallites," *Spectrochimica Acta Part A: Molecular and Biomolecular Spectroscopy*, vol. 130, pp. 344-349, 2014.
- [44] A. Shivashankarappa and K. Sanjay, "Study on Biological Synthesis of Cadmium Sulfide Nanoparticles by *Bacillus licheniformis* and Its Antimicrobial Properties against Food Borne Pathogens," *Nanoscience and Nanotechnology Research*, vol. 3, pp. 6-15, 2015.
- [45] P. Vos, G. Garrity, D. Jones, N. R. Krieg, W. Ludwig, F. A. Rainey, et al., *Bergey's Manual of Systematic Bacteriology: Volume 3: The Firmicutes* vol. 3: Springer Science & Business Media, 2011.
- [46] W. G. Weisburg, S. M. Barns, D. A. Pelletier, and D. J. Lane, "16S ribosomal DNA amplification for phylogenetic study," *Journal of bacteriology*, vol. 173, pp. 697-703, 1991.
- [47] A.-L. Reysenbach, L. J. Giver, G. S. Wickham, and N. R. Pace, "Differential amplification of rRNA genes by polymerase chain reaction," *Applied and Environmental Microbiology*, vol. 58, pp. 3417-3418, 1992.
- [48] S. F. Altschul, T. L. Madden, A. A. Schäffer, J. Zhang, Z. Zhang, W. Miller, et al., "Gapped BLAST and PSI-BLAST: a new generation of protein database search programs," *Nucleic acids research*, vol. 25, pp. 3389-3402, 1997.
- [49] J. D. Thompson, T. J. Gibson, F. Plewniak, F. Jeanmougin, and D. G. Higgins, "The CLUSTAL_X

windows interface: flexible strategies for multiple sequence alignment aided by quality analysis tools," *Nucleic acids research*, vol. 25, pp. 4876-4882, 1997.

- [50] K. Tamura, D. Peterson, N. Peterson, G. Stecher, M. Nei, and S. Kumar, "MEGA5: molecular evolutionary genetics analysis using maximum likelihood, evolutionary distance, and maximum parsimony methods," *Molecular biology and evolution*, vol. 28, pp. 2731-2739, 2011.
- [51] A. Ahmad, P. Mukherjee, S. Senapati, D. Mandal, M. I. Khan, R. Kumar, et al., "Extracellular biosynthesis of silver nanoparticles using the fungus *Fusarium oxysporum*," *Colloids and Surfaces B: Biointerfaces*, vol. 28, pp. 313-318, 2003.
- [52] A. Bauer, W. Kirby, J. C. Sherris, and M. Turck, "Antibiotic susceptibility testing by a standardized single disk method," *American journal of clinical pathology*, vol. 45, p. 493, 1966.
- [53] S. Gurunathan, J. W. Han, D.-N. Kwon, and J.-H. Kim, "Enhanced antibacterial and anti-biofilm activities of silver nanoparticles against Gram-negative and Gram-positive bacteria," *Nanoscale research letters*, vol. 9, p. 1, 2014.
- [54] I. Wiegand, K. Hilpert, and R. E. Hancock, "Agar and broth dilution methods to determine the minimal inhibitory concentration (MIC) of antimicrobial substances," *Nature protocols*, vol. 3, pp. 163-175, 2008.
- [55] W.-R. Li, X.-B. Xie, Q.-S. Shi, H.-Y. Zeng, O.-Y. You-Sheng, and Y.-B. Chen, "Antibacterial activity and mechanism of silver nanoparticles on *Escherichia coli*," *Applied microbiology and biotechnology*, vol. 85, pp. 1115-1122, 2010.
- [56] G. D. Christensen, W. Simpson, J. Younger, L. Baddour, F. Barrett, D. Melton, et al., "Adherence of coagulase-negative staphylococci to plastic tissue culture plates: a quantitative model for the adherence of staphylococci to medical devices," *Journal of clinical microbiology*, vol. 22, pp. 996-1006, 1985.
- [57] S. Stepanović, D. Vuković, I. Dakić, B. Savić, and M. Švabić-Vlahović, "A modified microtiter-plate test for quantification of staphylococcal biofilm formation," *Journal of microbiological methods*, vol. 40, pp. 175-179, 2000.
- [58] S. Javed, A. Sarwar, M. Tassarar, and M. Faisal, "Conversion of selenite to elemental selenium by indigenous bacteria isolated from polluted areas," *Chemical Speciation & Bioavailability*, vol. 27, pp. 162-168, 2015.
- [59] A. Ahmad, S. Senapati, M. I. Khan, R. Kumar, R. Ramani, V. Srinivas, et al., "Intracellular synthesis of gold nanoparticles by a novel alkalotolerant actinomycete, *Rhodococcus* species," *Nanotechnology*, vol. 14, p. 824, 2003.

- [60] N. Srivastava and M. Mukhopadhyay, "Biosynthesis and structural characterization of selenium nanoparticles using *Gliocladium roseum*," *Journal of Cluster Science*, vol. 26, pp. 1473-1482, 2015.
- [61] V. Gürtler and V. A. Stanisich, "New approaches to typing and identification of bacteria using the 16S-23S rDNA spacer region," *Microbiology*, vol. 142, pp. 3-16, 1996.
- [62] S. Tork, M. Aly, and L. Nawar, "Biochemical and molecular characterization of a new local keratinase producing *Pseudomonas* sp., MS21," *Asian J Biotechnol*, vol. 2, pp. 1-13, 2010.
- [63] M. A. Azcárate-Peril and R. R. Raya, "Methods for plasmid and genomic DNA isolation from *Lactobacilli*," *Methods in Biotechnology*, vol. 14, pp. 135-140, 2001.
- [64] M. Shakibaie, H. Forootanfar, Y. Golkari, T. Mohammadi-Khorsand, and M. R. Shakibaie, "Anti-biofilm activity of biogenic selenium nanoparticles and selenium dioxide against clinical isolates of *Staphylococcus aureus*, *Pseudomonas aeruginosa*, and *Proteus mirabilis*," *Journal of Trace Elements in Medicine and Biology*, vol. 29, pp. 235-241, 2015.
- [65] M. Joshi, A. Bhattacharyya, and S. W. Ali, "Characterization techniques for nanotechnology applications in textiles," 2008.
- [66] T. Hemalatha, G. Krithiga, B. S. Kumar, and T. P. Sastry, "Preparation and Characterization of Hydroxyapatite-Coated Selenium Nanoparticles and their Interaction with Osteosarcoma (SaOS-2) Cells," *Acta Metallurgica Sinica (English Letters)*, vol. 27, pp. 1152-1158, 2014.
- [67] B. Nair and T. Pradeep, "Coalescence of nanoclusters and formation of submicron crystallites assisted by *Lactobacillus* strains," *Crystal Growth & Design*, vol. 2, pp. 293-298, 2002.
- [68] Z.-H. Lin and C. C. Wang, "Evidence on the size-dependent absorption spectral evolution of selenium nanoparticles," *Materials Chemistry and Physics*, vol. 92, pp. 591-594, 2005.
- [69] A. Husen and K. S. Siddiqi, "Plants and microbes assisted selenium nanoparticles: characterization and application," *Journal of nanobiotechnology*, vol. 12, p. 28, 2014.
- [70] A. Hnain, J. Brooks, and D. D. Lefebvre, "The synthesis of elemental selenium particles by *Synechococcus leopoliensis*," *Applied microbiology and biotechnology*, vol. 97, pp. 10511-10519, 2013.
- [71] S. R. Santanu Sasidharan, Balakrishnaraja.R, "BIOSYNTHESIS OF SELENIUM NANOPARTICLES USING CITRUS RETICULATA PEEL EXTRACT," *colloids and Surfaces* vol. 4, pp. 196–201, 2011.
- [72] N. Srivastava and M. Mukhopadhyay, "Biosynthesis and structural characterization of selenium

- nanoparticles mediated by *Zooglea ramigera*," Powder technology, vol. 244, pp. 26-29, 2013.
- [73] A. R. Ingole, S. R. Thakare, N. Khati, A. V. Wankhade, and D. Burghate, "Green synthesis of selenium nanoparticles under ambient condition," Chalcogenide Lett, vol. 7, pp. 485-489, 2010.
- [74] R. R. Mishra, S. Prajapati, J. Das, T. K. Dangar, N. Das, and H. Thatoi, "Reduction of selenite to red elemental selenium by moderately halotolerant *Bacillus megaterium* strains isolated from Bhitarkanika mangrove soil and characterization of reduced product," Chemosphere, vol. 84, pp. 1231-1237, 2011.
- [75] M. Mukherje, "In vitro antimicrobial activity of polyacrylamide doped magnetic iron oxide nanoparticles," Int J Mater Mech Manuf, vol. 2, pp. 64-66, 2014.
- [76] J. Huang, Q. Li, D. Sun, Y. Lu, Y. Su, X. Yang, et al., "Biosynthesis of silver and gold nanoparticles by novel sundried *Cinnamomum camphora* leaf," Nanotechnology, vol. 18, p. 105104, 2007.
- [77] A. Tani, S. Kato, Y. Kajii, M. Wilkinson, S. Owen, and N. Hewitt, "A proton transfer reaction mass spectrometry based system for determining plant uptake of volatile organic compounds," Atmospheric Environment, vol. 41, pp. 1736-1746, 2007.
- [78] K. S. Prasad and K. Selvaraj, "Biogenic synthesis of selenium nanoparticles and their effect on As (III)-induced toxicity on human lymphocytes," Biological trace element research, vol. 157, pp. 275-283, 2014.
- [79] J. Díaz-Visurraga, C. Daza, C. Pozo, A. Becerra, C. von Plessing, and A. García, "Study on antibacterial alginate-stabilized copper nanoparticles by FT-IR and 2D-IR correlation spectroscopy," Int J Nanomedicine, vol. 7, pp. 3597-3612, 2012.
- [80] W. Zhang, Z. Chen, H. Liu, L. Zhang, P. Gao, and D. Li, "Biosynthesis and structural characteristics of selenium nanoparticles by *Pseudomonas alcaliphila*," Colloids and Surfaces B: Biointerfaces, vol. 88, pp. 196-201, 2011.
- [81] M. Lenz, B. Kolvenbach, B. Gygax, S. Moes, and P. F. Corvini, "Shedding light on selenium biomineralization: proteins associated with bionanominerals," Applied and environmental microbiology, pp. AEM. 01713-10, 2011.
- [82] J. Dobias, E. I. Suvorova, and R. Bernier-Latmani, "Role of proteins in controlling selenium nanoparticle size," Nanotechnology, vol. 22, p. 195605, 2011.
- [83] M. Yasuyuki, K. Kunihiro, S. Kurissery, N. Kanavillil, Y. Sato, and Y. Kikuchi, "Antibacterial properties of nine pure metals: a laboratory study using *Staphylococcus aureus* and *Escherichia coli*," Biofouling, vol. 26, pp. 851-858, 2010.
- [84] P. Nagajyothi and K. Lee, "Synthesis of plant-mediated silver nanoparticles using *Dioscorea batatas*

- rhizome extract and evaluation of their antimicrobial activities," *Journal of nanomaterials*, vol. 2011, p. 49, 2011.
- [85] G. Krishna, S. S. Kumar, V. Pranitha, M. Alha, and S. Charaya, "Biogenic synthesis of silver nanoparticles and their synergistic effect with antibiotics: A study against salmonella SP," *International journal of pharmacy and pharmaceutical Sciences*, vol. 7, pp. 84-88, 2015.
- [86] X. Huang, X. Chen, Q. Chen, Q. Yu, D. Sun, and J. Liu, "Investigation of functional selenium nanoparticles as potent antimicrobial agents against superbugs," *Acta biomaterialia*, vol. 30, pp. 397-407, 2016.
- [87] Y. Zhou, Y. Kong, S. Kundu, J. D. Cirillo, and H. Liang, "Antibacterial activities of gold and silver nanoparticles against *Escherichia coli* and *Bacillus Calmette-Guérin*," *Journal of Nanobiotechnology*, vol. 10, p. 1, 2012.
- [88] J. T. Seil and T. J. Webster, "Antimicrobial applications of nanotechnology: methods and literature," *Int J Nanomedicine*, vol. 7, pp. 2767-2781, 2012.
- [89] H.-S. Joo and M. Otto, "Molecular basis of in vivo biofilm formation by bacterial pathogens," *Chemistry & biology*, vol. 19, pp. 1503-1513, 2012.
- [90] E. Cremonini, E. Zonaro, M. Donini, S. Lampis, M. Boaretti, S. Dusi, et al., "Biogenic selenium nanoparticles: characterization, antimicrobial activity and effects on human dendritic cells and fibroblasts," *Microbial Biotechnology*, 2016.
- [91] J. S. Webb, L. S. Thompson, S. James, T. Charlton, T. Tolker-Nielsen, B. Koch, et al., "Cell death in *Pseudomonas aeruginosa* biofilm development," *Journal of bacteriology*, vol. 185, pp. 4585-4592, 2003.
- [92] E. Zonaro, S. Lampis, R. J. Turner, S. J. S. Qazi, and G. Vallini, "Biogenic selenium and tellurium nanoparticles synthesized by environmental microbial isolates efficaciously inhibit bacterial planktonic cultures and biofilms," *Frontiers in microbiology*, vol. 6, p. 584, 2015.
- [93] K. A. A. A. Rahim and A. M. A. Mohamed, "Bactericidal and antibiotic synergistic effect of nanosilver against methicillin-resistant *Staphylococcus aureus*," *Jundishapur journal of microbiology*, vol. 8, 2015.